National School on Neutron and X-ray Scattering

Argonne and Oak Ridge National laboratories

X-ray and Neutron Reflectometry

August 20, 2013

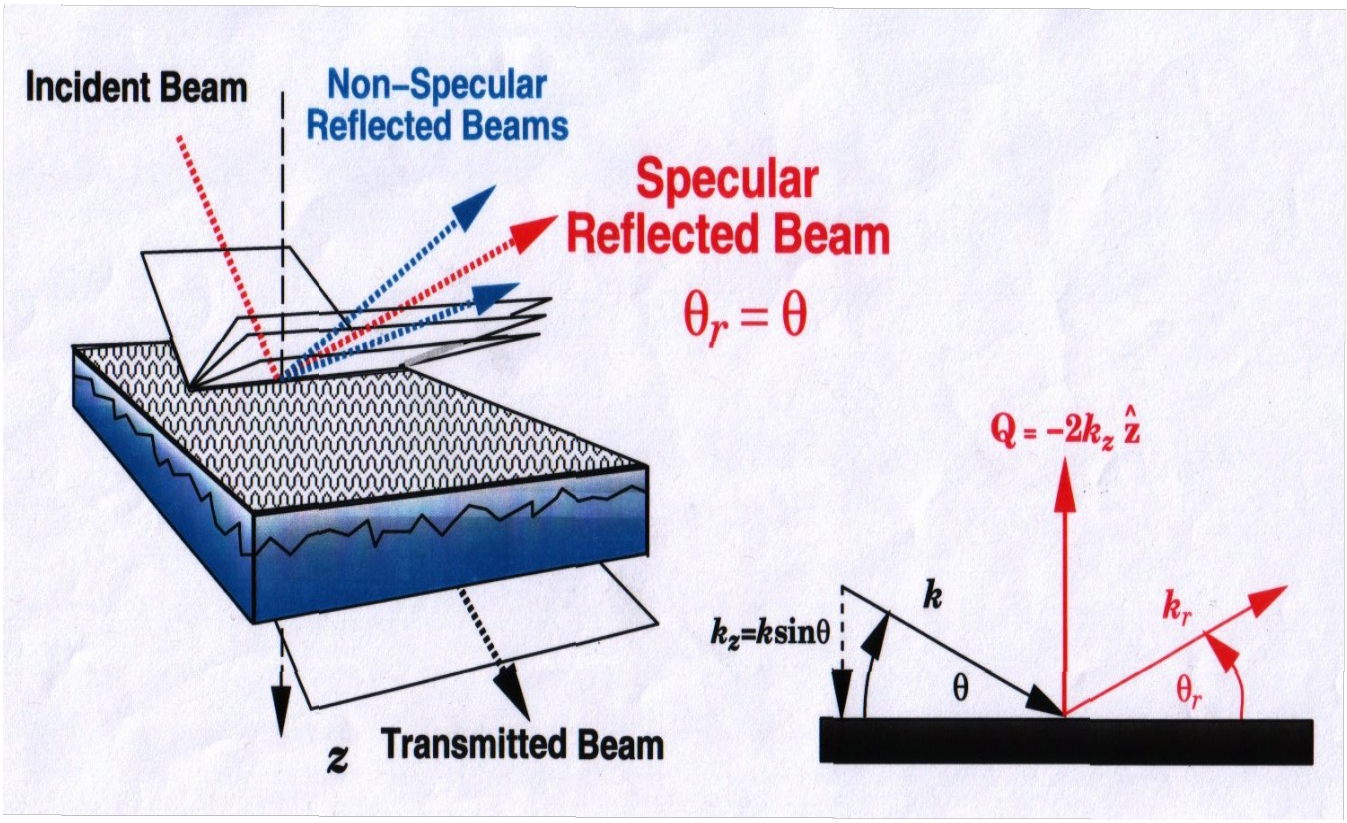

(Figure courtesy of Norm Berk)

C.F.Majkrzak, *NIST Center for Neutron Research*, Gaithersburg, MD

Part 1: Basic Reflectometry Concepts

<> diffraction versus real space imaging

<> probing structure beneath the surface boundary

<> wave/particle behavior

<> coherence length -- plane waves and wave packets

<> specular reflection from a flat object

<> scattering length density (SLD) depth profiles

<> spatial and Q resolutions

<> non-specular scattering

Principal Uses and Advantages of Neutron Reflectometry:

* For the specular condition, provides the chemical (isotopic) scattering length density (SLD) depth profile along the surface normal with a spatial resolution approaching half a nanometer.

* With polarized neutrons, provides the *vector* magnetization depth profile of a ferromagnetic material.

* Isotopic contrast, particularly applicable to hydrogen and deuterium.

* A non-destructive probe which can penetrate macroscopic distances through single crystalline substrates, making possible reflection studies of films in contact with liquids within a closed cell.

* As a consequence of the relatively weak interaction between the neutron and material, a remarkably accurate theoretical description of the reflection process and quantitative analysis of the data is possible, although the Born approximation is often not valid and an “exact” or “dynamical” formulation is required.

Importance of Sample System Preparation

> The great success in using neutron reflection/diffraction to study thin film systems of hard condensed matter, in particular the structures and fundamental interactions in magnetic materials, is largely due to the ability to tailor, with atomic-layer accuracy and precision, single-crystalline, layered sandwiches and superlattices (using vapor deposition techniques such as molecular beam epitaxy in ultra-high vacuum). Advances in film deposition techniques and lithography continue at a remarkable rate.

> Similarly, neutron reflectometry in principle can be applied as a probe to further our understanding of the structure and function of molecules in lipid membranes, of relevance in biology and bioengineering, when comparable control over the fabrication of model systems is achieved. Great progress has been made toward realizing this goal in practice. However, we are still at a relatively early stage of development in our ability to engineer soft condensed matter films on atomic and nanometer scales. Progress can be expected as efforts in creating and manipulating membrane / molecular systems accelerates.

> Employing phase-sensitive methods in reflectivity measurements ensures a unique scattering length density (SLD) depth profile. Additional application of hydrogen / deuterium substitution techniques and comparison with molecular dynamics calculations assures a correspondingly high degree of certainty of obtaining an unambiguous chemical composition depth profile.

Why is specular neutron reflectometry so special?

<> Neutron reflectometry (NR) is a valuable probe of the structure of both hard and soft condensed matter in thin film or multilayered form -- particularly for hydrogenous and magnetic materials. NR can see *beneath* the surface and provide quantitative structural information from *everywhere within* the film on a nanometer scale.

<> Both “forward” and “inverse” scattering problems for specular neutron reflection are mathematically solvable, exactly, from first-principles quantum theory. The mathematically unique solutions are thus far only possible in one dimension and for non-absorbing potentials of finite extent.

<> Phase-sensitive neutron specular reflectometry, employing references, enables direct inversion of composite reflectivity data sets to yield a unique scattering length density depth profile for an “unknown” film of interest, without fitting or any adjustable parameters.

<> The spatial resolution and accuracy of the SLD profile thereby obtained is limited only by the statistical uncertainty in the measured reflected intensities and truncation of the reflectivity data sets at the maximum value of wavevector transfer attainable.

$$\text{Reflectivity} = \frac{\text{Number of reflected neutrons}}{\text{Number of incident neutrons}} = |r|^2$$

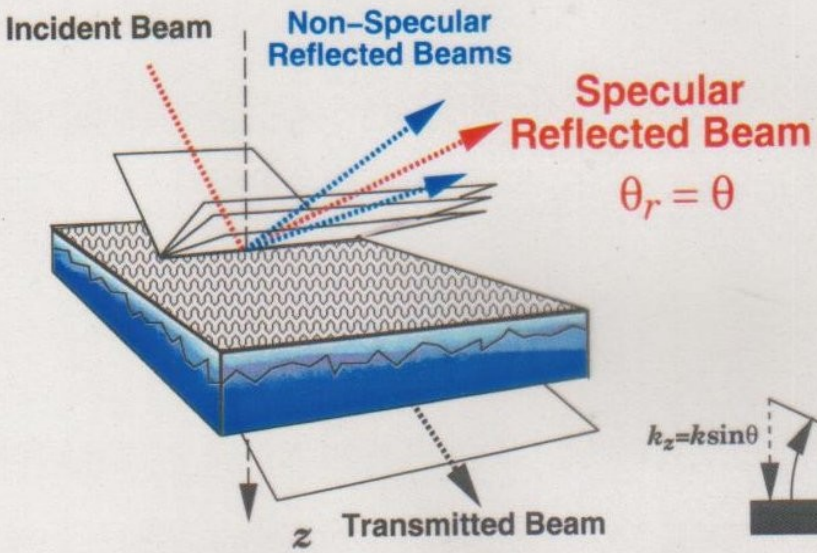

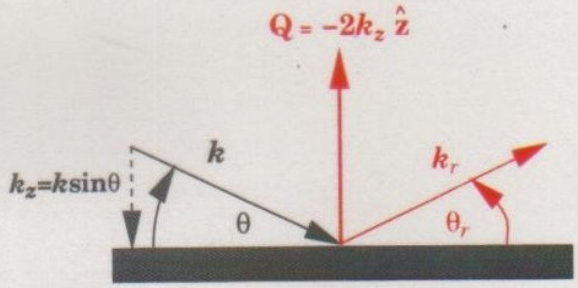

Specular reflection: $\bar{\rho}(z) = \langle\rho(x,y,z)\rangle_{xy}$

Non–Specular reflection: $\Delta\rho(x,y,z) = \rho(x,y,z) - \bar{\rho}(z)$

(AFTER N.F.BERK ET AL.)

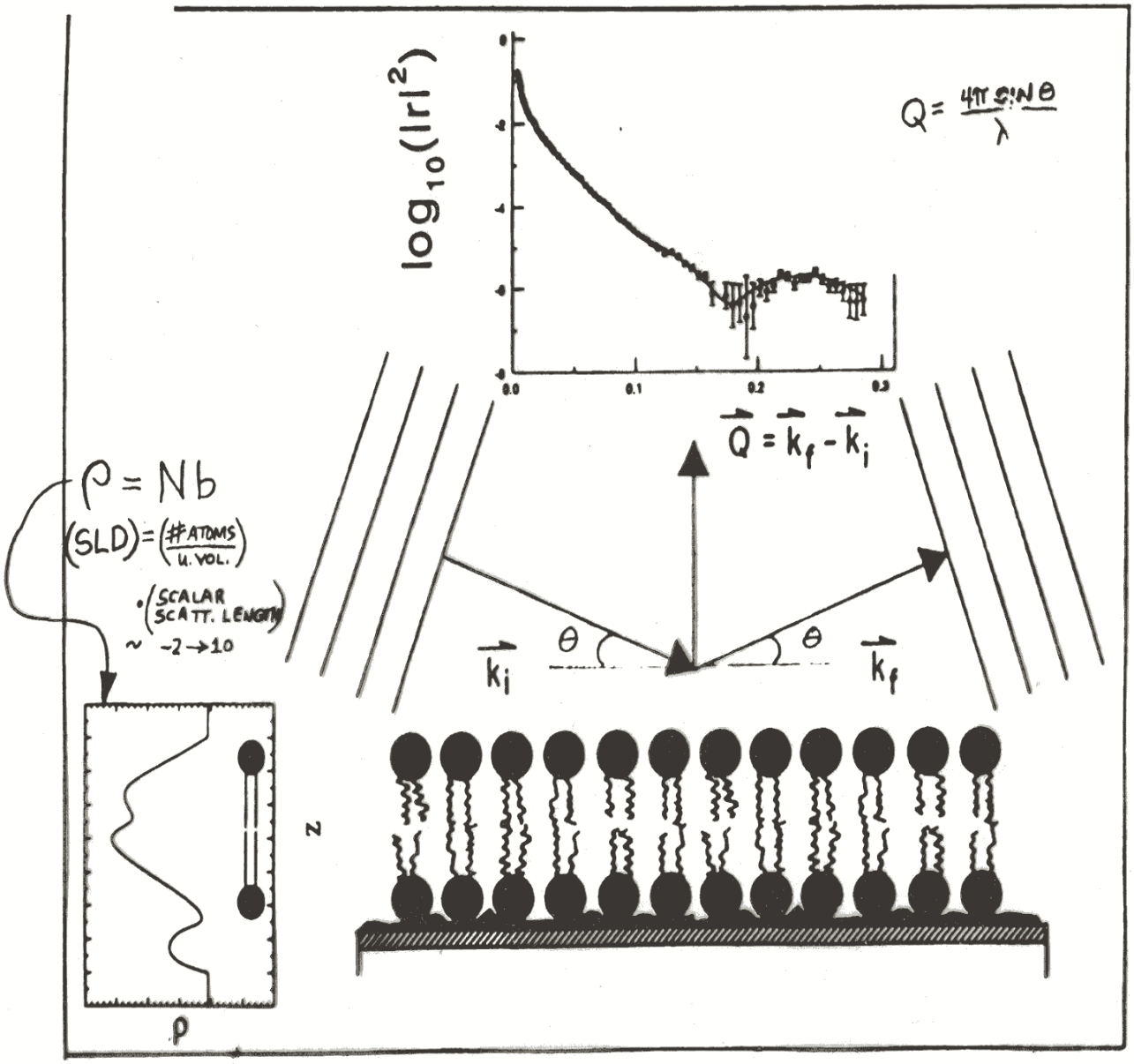
log10(|r|²)
Q = 4π sin θ / λ
Q = kf - ki
ρ = Nb
(SLD) = (# ATOMS / U. VOL.)
• (SCALAR SCATT. LENGTH)
~ -2 → 10
θ
θ
ki
kf
z
ρ

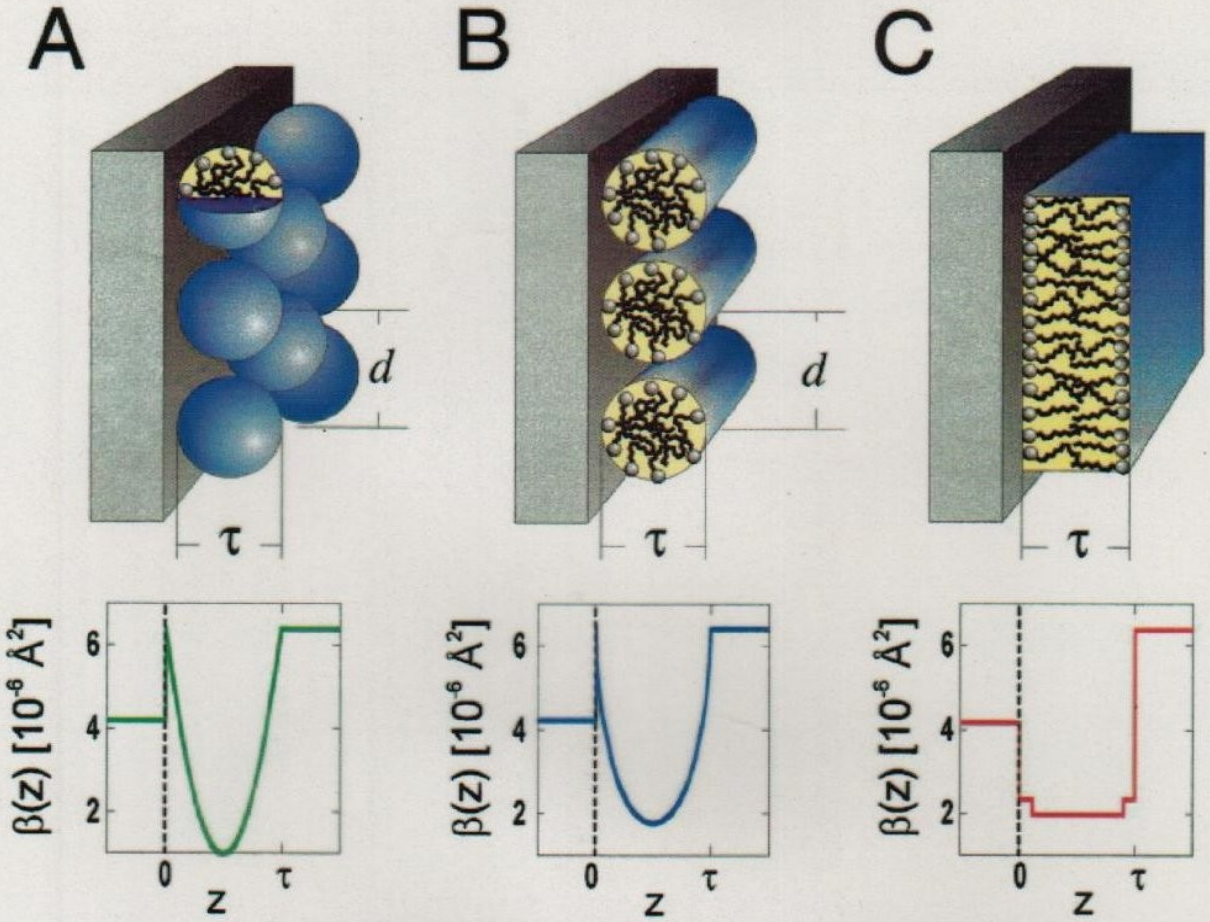

FIG. 1. (Color) Schematic diagram of adsorbed layer structures consisting of (A) spherical micelles, (B) cylindrical micelles, and (C) a bilayer, including the film thickness τ and interaggregate spacing d. Also shown are examples of neutron scattering length density profiles normal to the interface, $\beta(z)$, corresponding to each structure at the quartz/D_2O interface at a fractional surface coverage of 0.55. The head-group and alkyl tails of the surfactants have different scattering length densities, but because of the arrangement of the molecules this is only apparent in the bilayer $\beta(z)$.

single-crystal quartz block and reflected from the quartz-solution interface were recorded as a function of angle of incidence. The off-specular background, including any signal due to scattering from the bulk solution [15], was subtracted to give the reflection coefficient of the surfactant-coated interface. All solutions used were above their critical micelle or aggregation concentration, a condition which leads to a saturated adsorbed film at the solid-solution interface.

The cationic surfactant tetradecyltrimethylammonium bromide (TTAB) forms nearly spherical micellar aggregates consisting of approximately 80 molecules in bulk solution. Small angle neutron-scattering measurements [16] give mi-

FIG. 2. 200×200-nm^2 AFM tip deflection images of (A) spherical TTAB aggregates adsorbed onto quartz from water solution, (B) cylindrical TTAB aggregates adsorbed onto quartz from an aqueous 200mM NaBr solution, and (C) planar DDAB bilayer adsorbed onto quartz from water solution. Long-wavelength undulations visible in (B) and (C) arise from roughness in the underlying quartz.

THE NEUTRON AS A PLANE WAVE PROPAGATING IN FREE SPACE

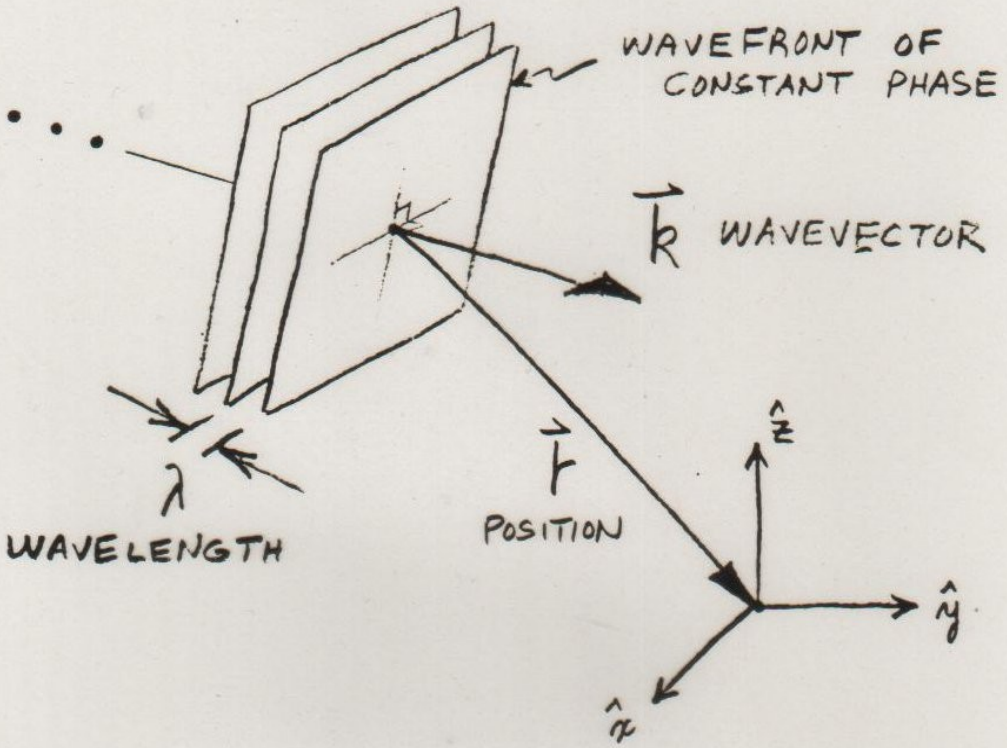

WAVEFUNCTION

$$\Psi \propto e^{i\vec{k}_0 \cdot \vec{r}}$$

$$\begin{cases} \vec{k}_0 = k_{0x}\hat{x} + k_{0y}\hat{y} + k_{0z}\hat{z} \\ \vec{r} = x\hat{x} + y\hat{y} + z\hat{z} \end{cases}$$

FOR $\vec{k}_0$ ALONG $\hat{z}$, FOR EXAMPLE,

$$\Psi \propto \cos(\underbrace{k_{0z} z}_{= \left(\frac{2\pi}{\lambda} z\right)}) + i \sin(k_{0z} z)$$

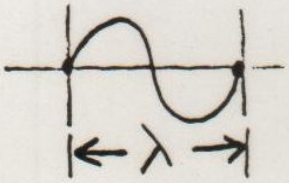

$|\Psi|^2 \propto$ PROBABILITY OF THE NEUTRON BEING THERE

FOR ELASTIC INTERACTIONS
TOTAL ENERGY OF THE
NEUTRON IS CONSTANT

TOTAL ENERGY = KINETIC ENERGY
+ POTENTIAL ENERGY

= CONSTANT

WAVE EQUATION OF MOTION
(SCHROEDINGER EQUATION)

$$\underbrace{\left[\frac{-\hbar^2}{2m}\nabla^2\right.}_{\text{K.E.}} + \underbrace{\left.V(\vec{r})\right]}_{\text{P.E.}}\Psi = \underbrace{E}_{\text{T.E.}}\Psi$$

$$\nabla^2 = \frac{\partial^2}{\partial x^2} + \frac{\partial^2}{\partial y^2} + \frac{\partial^2}{\partial z^2}$$

IN VACUUM

$$K.E._0 = \frac{\hbar^2 k_0^2}{2m}$$

IN THE CONTINUUM LIMIT

$$V(\vec{r}) = \frac{2\pi\hbar^2}{m} \sum_{j=1} N_j b_j = \frac{2\pi\hbar^2}{m}\rho$$

NUMBER OF ATOMS OF TYPE j PER UNIT VOLUME

COHERENT SCATTERING "LENGTH" OF ATOM j

$(b = \mathrm{Re}\,b + i\,\mathrm{Im}\,b)$

ρ = "SCATTERING LENGTH DENSITY" (SLD)

IN VACUUM:

$$E_0 = \frac{\hbar^2 k_0^2}{2m} + 0$$

IN A MATERIAL MEDIUM:

$$E = \frac{\hbar^2 k^2}{2m} + \frac{2\pi\hbar^2}{m}\rho$$

CONSERVATION OF ENERGY REQUIRES $E_0 = E$

$$\therefore \quad k^2 = k_0^2 - 4\pi\rho$$

THUS

$$\left[\nabla^2 + k^2\right]\Psi = 0$$

NOTE REFRACTIVE INDEX $n \equiv \frac{k}{k_0}$:

$$n^2 = 1 - \frac{4\pi\rho}{k_0^2}$$

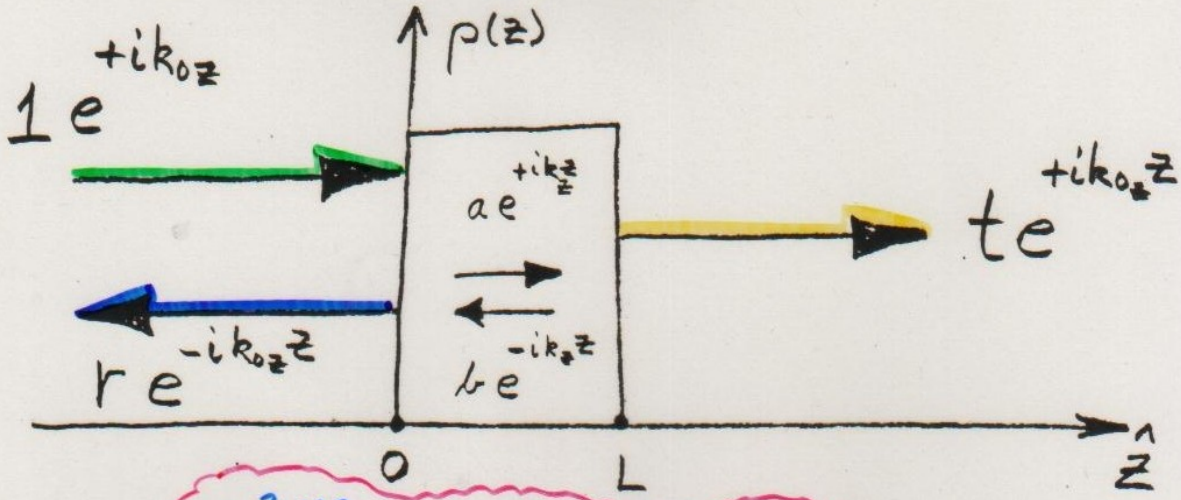

$$\frac{\partial^2 \psi(z)}{\partial z^2} + k_z^2 \psi(z) = 0$$

CONSERVATION OF MOMENTUM AND PARTICLE NUMBER REQUIRE THAT $\frac{\partial \psi(z)}{\partial z}$ AND $\psi(z)$

BE CONTINUOUS AT THE BOUNDARIES $z=0$ & $z=L$

$$\begin{pmatrix} t \\ it \end{pmatrix} e^{ik_{0z}L} = \begin{pmatrix} A & B \\ C & D \end{pmatrix} \begin{pmatrix} 1+r \\ i(1-r) \end{pmatrix}$$

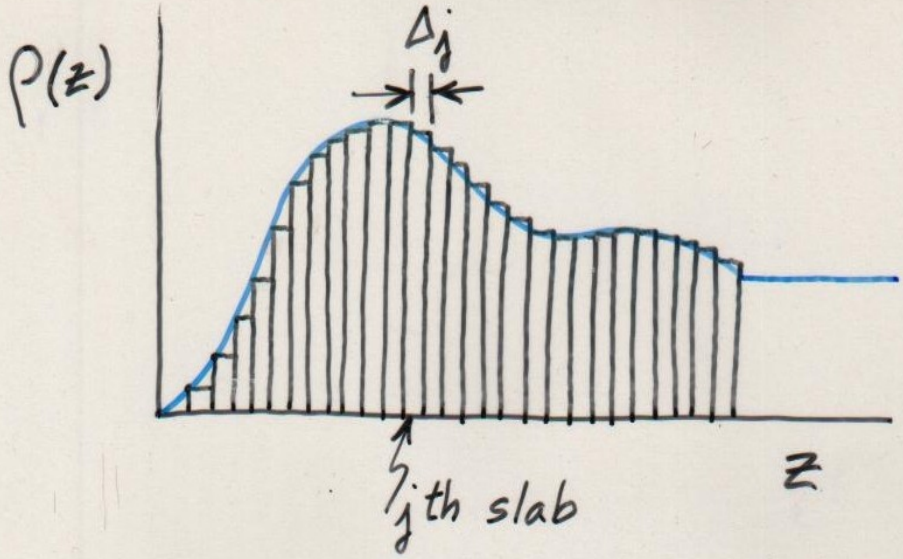

$$\begin{pmatrix} A & B \\ C & D \end{pmatrix} = \begin{pmatrix} a_N & b_N \\ c_N & d_N \end{pmatrix} \begin{pmatrix} a_{N-1} & b_{N-1} \\ c_{N-1} & d_{N-1} \end{pmatrix} \cdots \begin{pmatrix} a_2 & b_2 \\ c_2 & d_2 \end{pmatrix} \begin{pmatrix} a_1 & b_1 \\ c_1 & d_1 \end{pmatrix}$$

$$\begin{pmatrix} a_j & b_j \\ c_j & d_j \end{pmatrix} = \begin{pmatrix} \cos \delta_j & \frac{1}{n_{z_j}} \sin \delta_j \\ -n_{z_j} \sin \delta_j & \cos \delta_j \end{pmatrix}$$

$$\delta_j = k_{0z} n_{z_j} \Delta_j$$
$$= k_{z_j} \Delta_j$$

free film

Then, once we know $M_k(L)$:

$$\boxed{z=L} \qquad\qquad \boxed{z=0}$$

$$\begin{pmatrix} 1 \\ \mathrm{i} \end{pmatrix} t(k)\mathrm{e}^{\mathrm{i}kL} = \begin{pmatrix} A_k(L) & B_k(L) \\ C_k(L) & D_k(L) \end{pmatrix} \begin{pmatrix} 1+r(k) \\ \mathrm{i}[1-r(k)] \end{pmatrix}$$

$$\boxed{r = \frac{B+C+\mathrm{i}(D-A)}{B-C+\mathrm{i}(D+A)}}$$

$$t = \frac{2\mathrm{i}\mathrm{e}^{-\mathrm{i}kL}}{B-C+\mathrm{i}(D+A)}$$

$$R = |r|^2 = \frac{\Sigma-2}{\Sigma+2}, \quad \Sigma = \mathrm{A}^2 + \mathrm{B}^2 + \mathrm{C}^2 + \mathrm{D}^2$$

(Courtesy of Norm Berk)

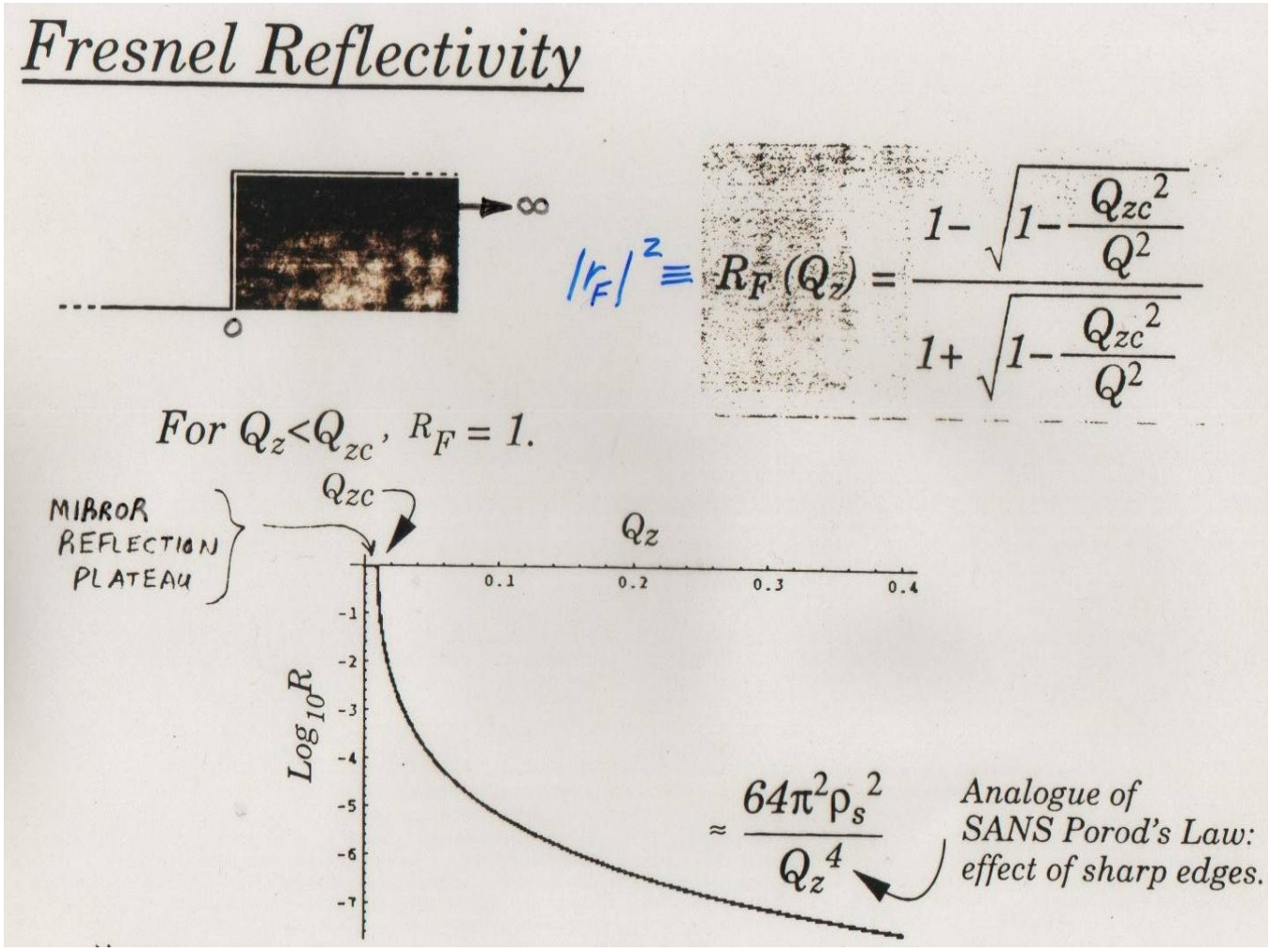

Qzc = SQRT(16*pi*rho) (Courtesy of Norm Berk)

"Soft" substrate

Smooth transition:
interlayer diffusion roughness

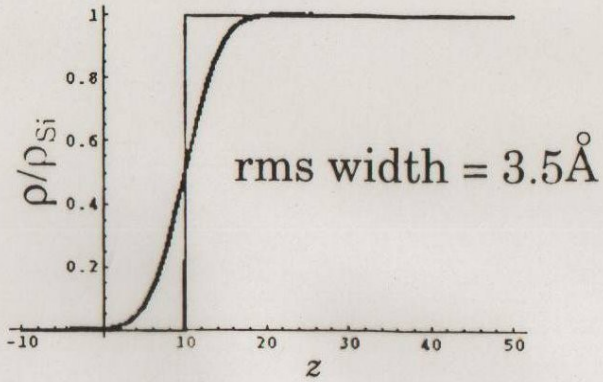

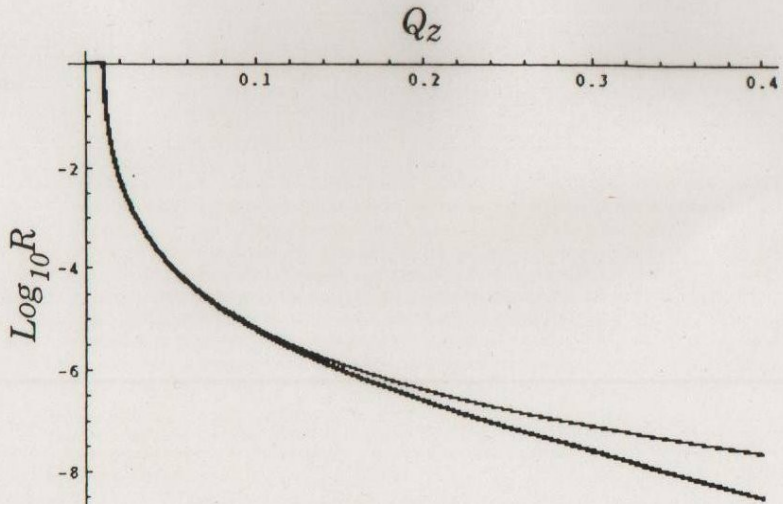

(N.F. BERK)

Uniform slab

$\rho = 2.07\ 10^{-6}\text{Å}^{-2}$

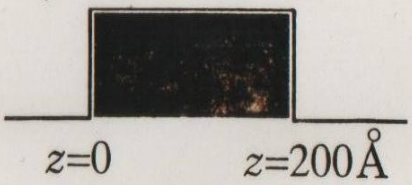

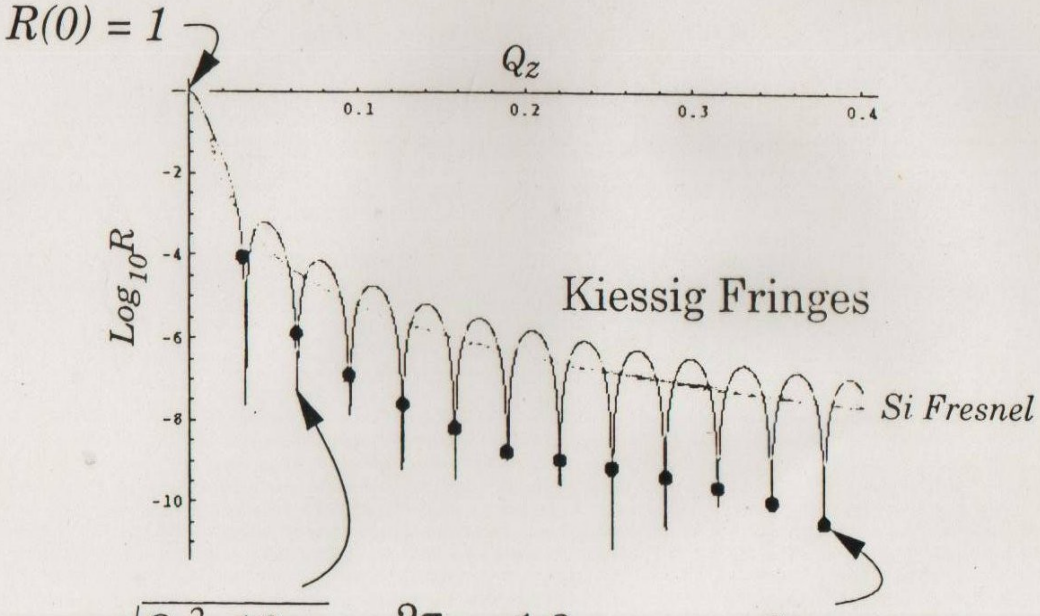

$\sqrt{Q_z^2 - 16\pi\rho} = \frac{2\pi}{L} m=1,2,...$

$\frac{2\pi}{L} m=1,2,...$

(*Kinematical*)

(N.F. BERK)

Multilayer on Si

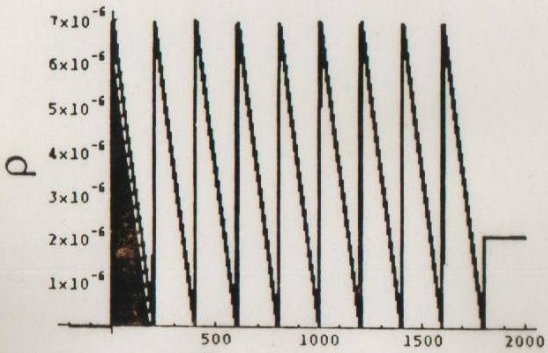

$D = 200\text{Å}$ z $L = 9 \times 200\text{Å}$

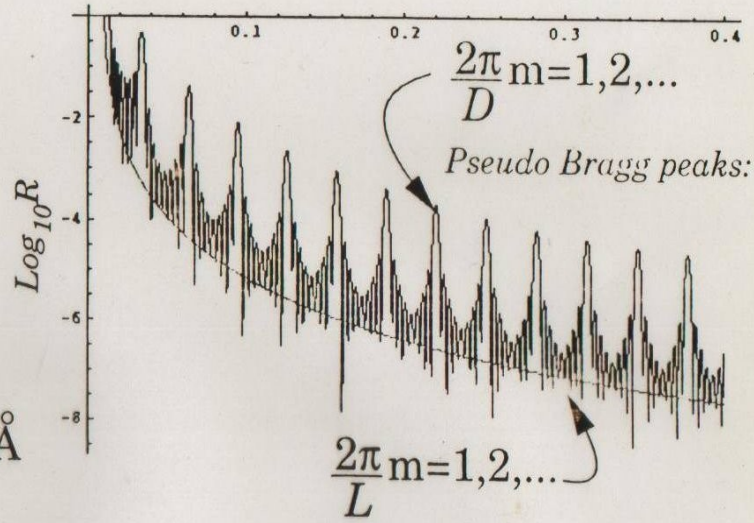

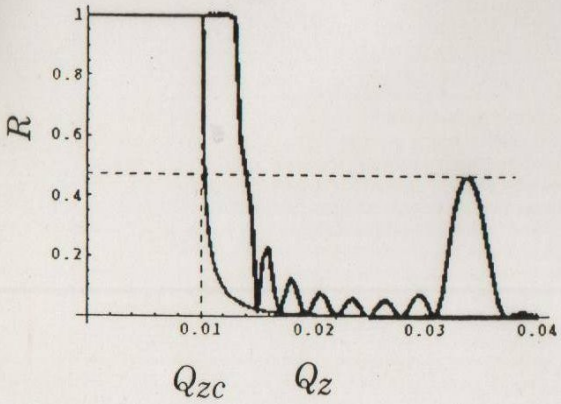

$L = 18 \times 200\text{Å}$

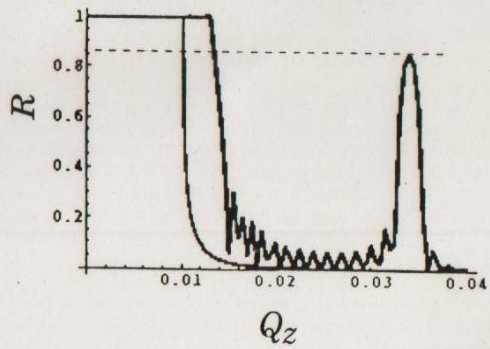

(N.F. BERK)

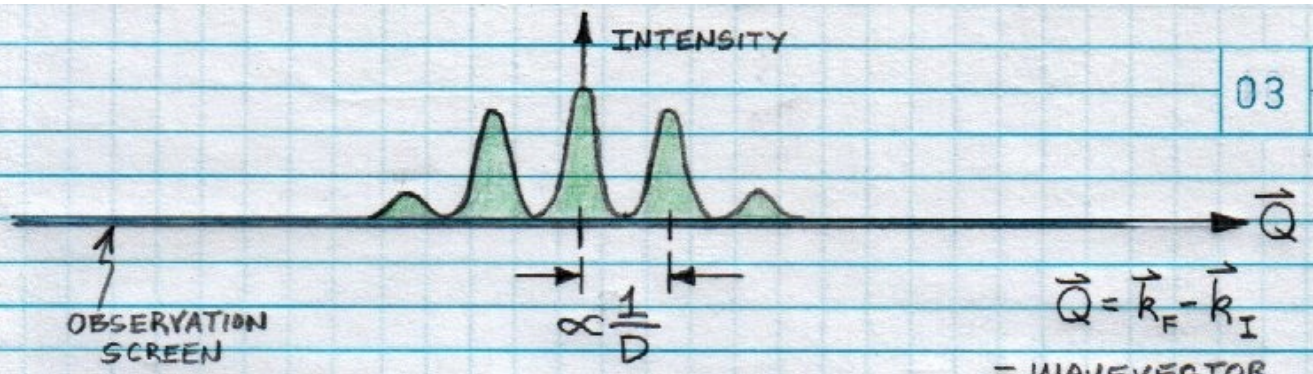

$\vec{Q} = \vec{k}_F - \vec{k}_I$

= WAVEVECTOR TRANSFER

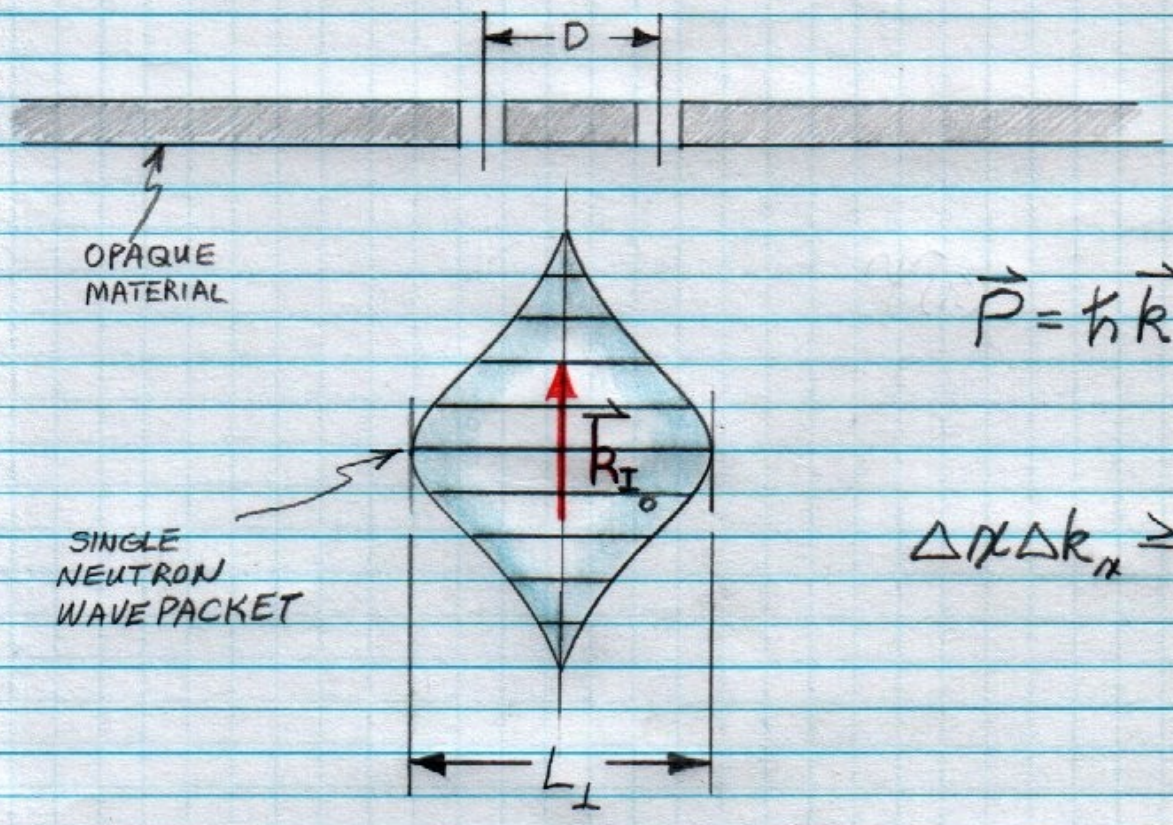

$\vec{P} = \hbar \vec{k}$

$\Delta x \Delta k_x \geq 1$

$$\Psi(\vec{r}) = \left(\frac{1}{2\pi}\right)^{3/2} \iiint_{-\infty}^{+\infty} d\vec{k}\, \phi(\vec{k})\, e^{+i\vec{k}\cdot\vec{r}}$$

$$\phi(\vec{k}) = \left(\frac{1}{2\pi}\right)^{3/2} \iiint_{-\infty}^{+\infty} d\vec{r}\, \Psi(\vec{r})\, e^{-i\vec{k}\cdot\vec{r}}$$

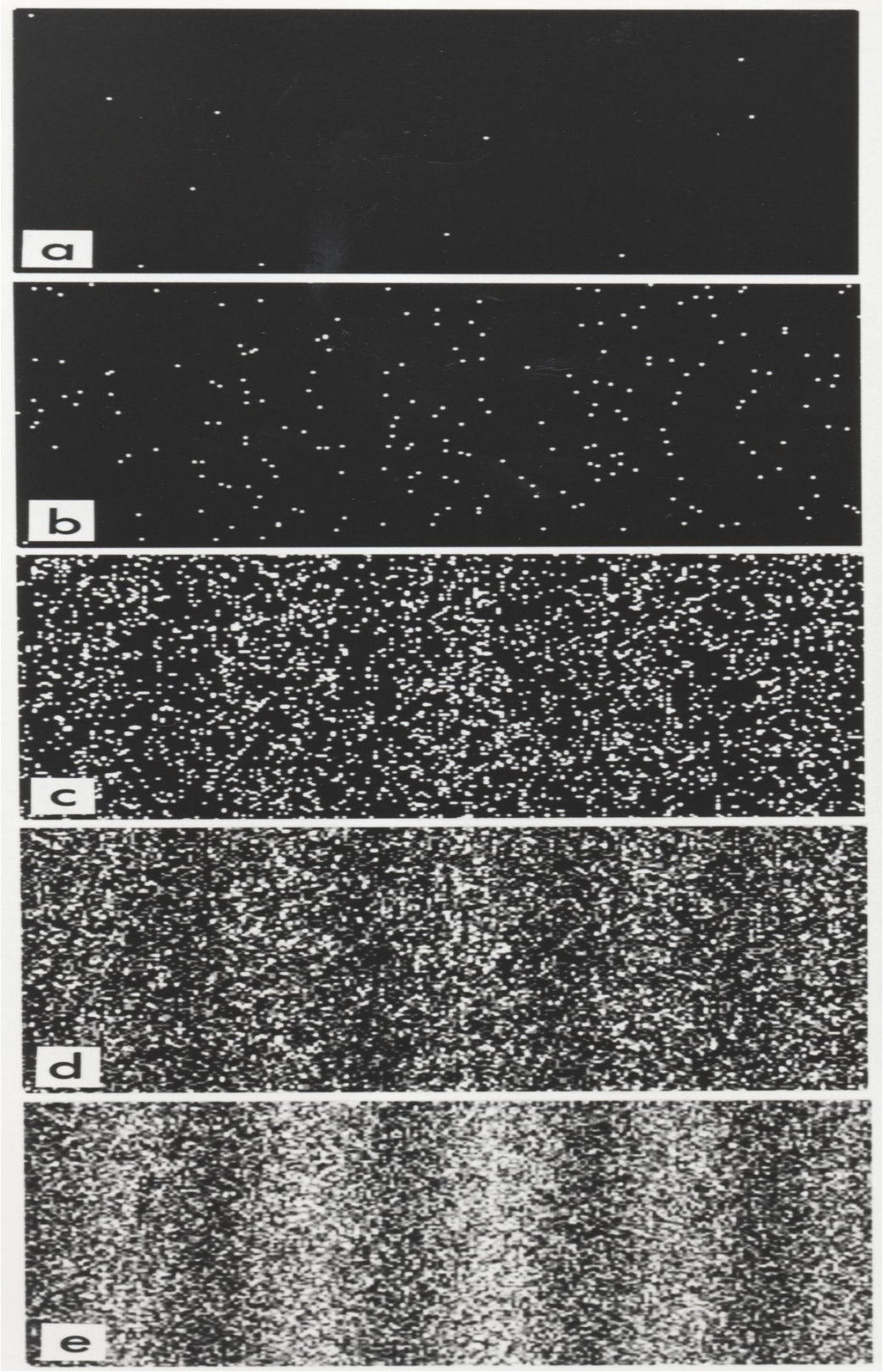

Electron diffraction pattern from a double slit -- one electron at a time (courtesy of Dr. Tanamura via Wikipedia.org).

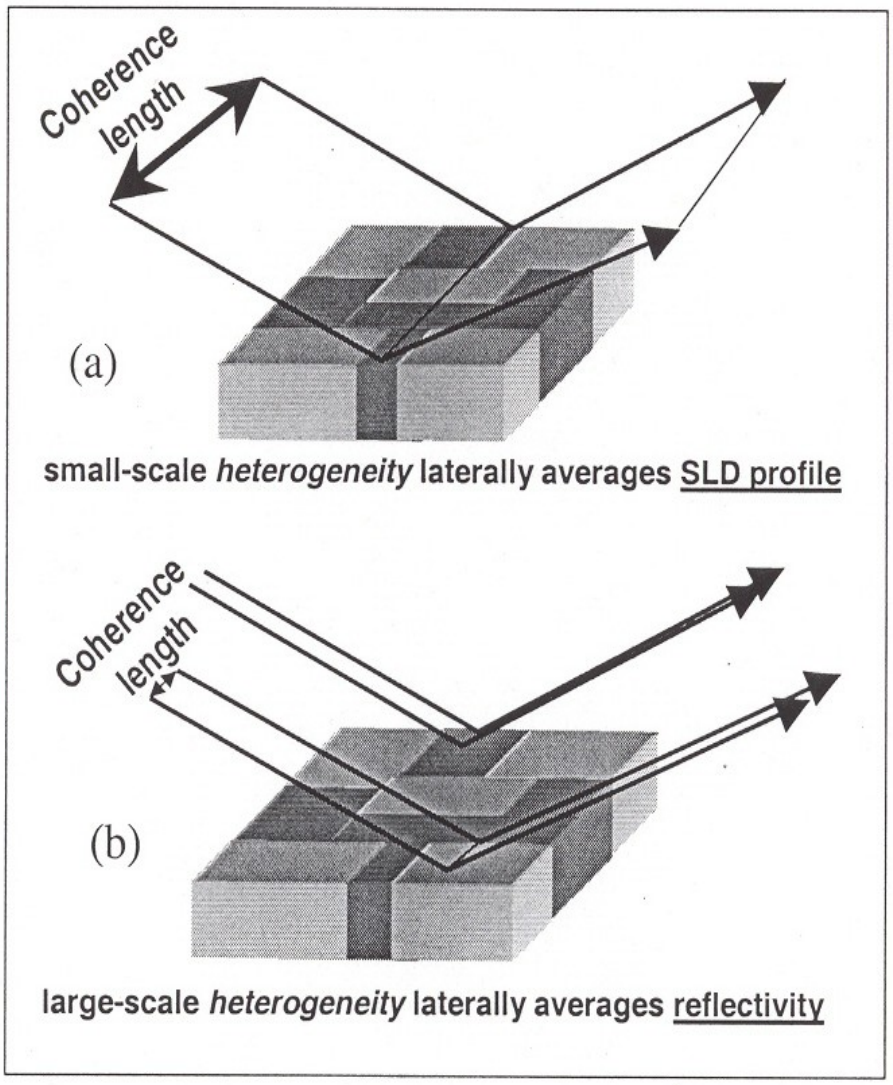

$$r = (4\pi / (iQ)) \int_{-\infty}^{+\infty} \psi_{kz}(z) \langle \rho(x,y,z) \rangle_{x,y} e^{ikz} dz$$

$$\langle \rho(x,y,z) \rangle_{x,y} = (1/A) \iint_{-\infty}^{+\infty} \rho(x,y,z) \, dxdy$$

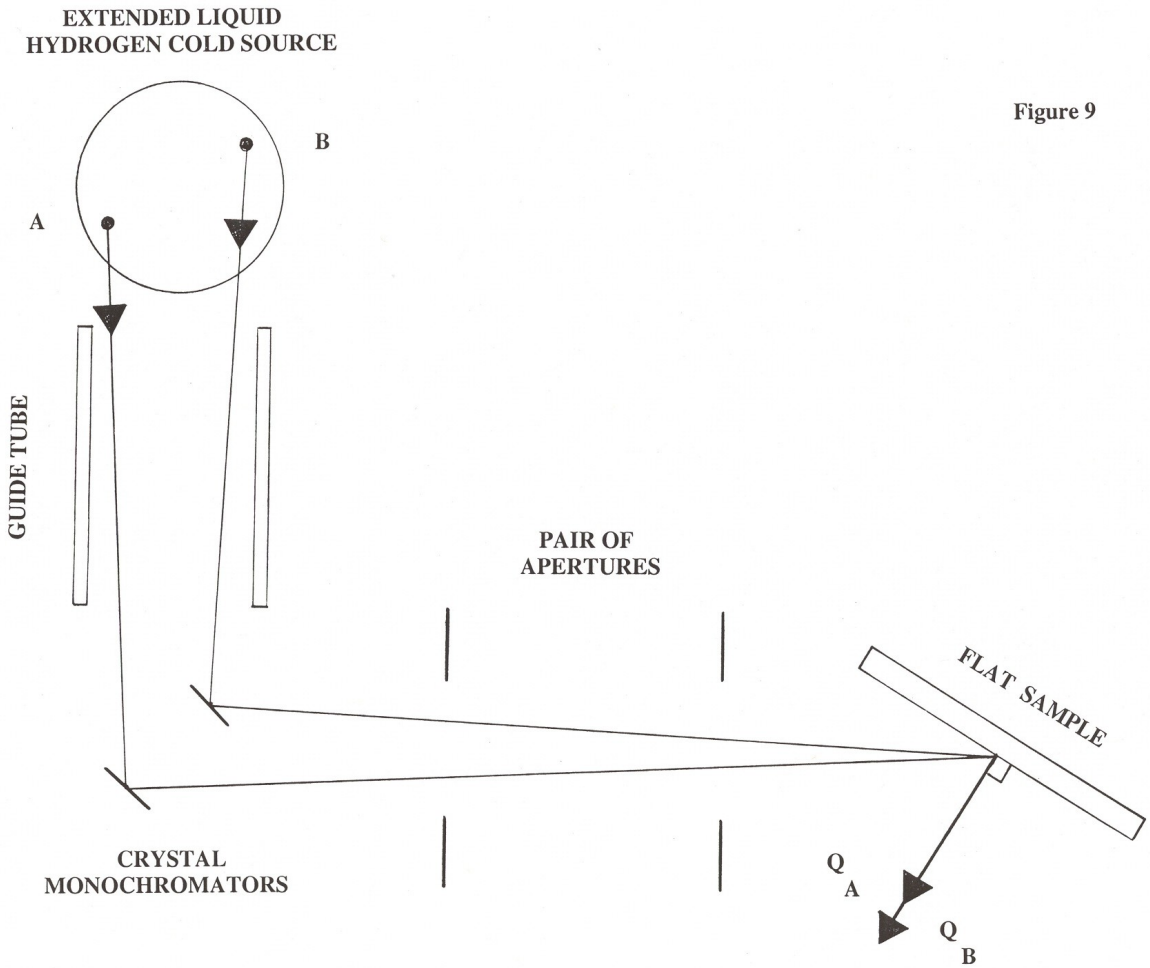
EXTENDED LIQUID
HYDROGEN COLD SOURCE
B
A
GUIDE TUBE
PAIR OF
APERTURES
FLAT SAMPLE
CRYSTAL
MONOCHROMATORS
Q A
Q B

Figure 9

Figure 13

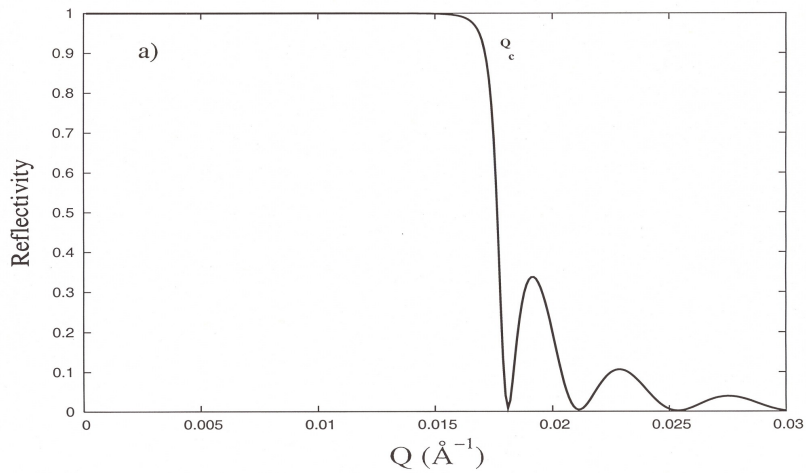

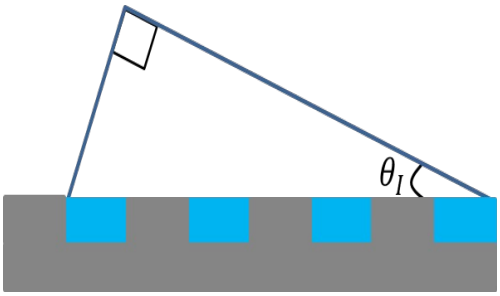

Figure 13

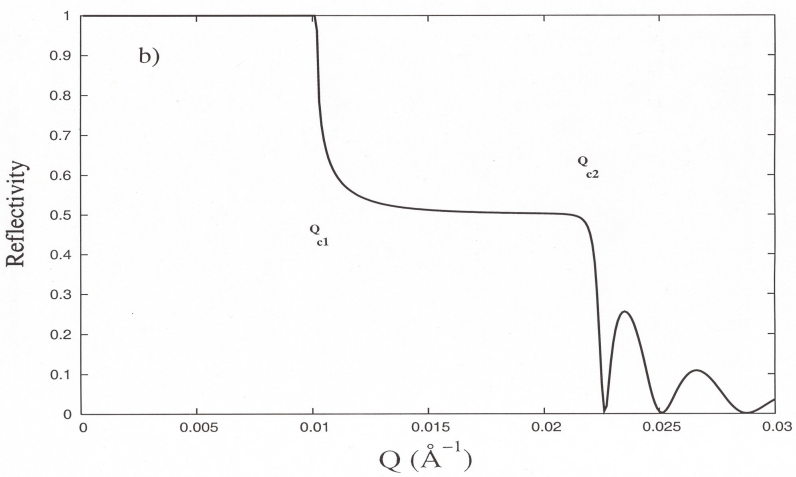

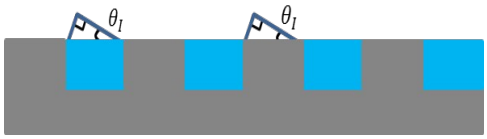

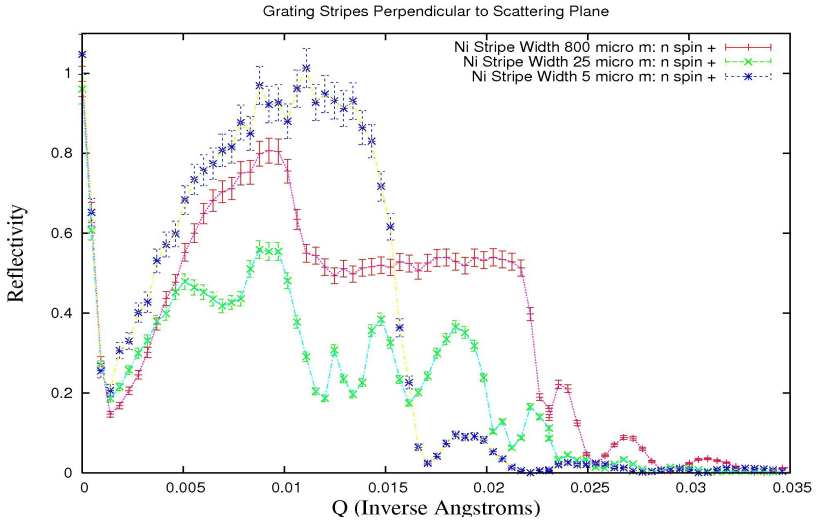

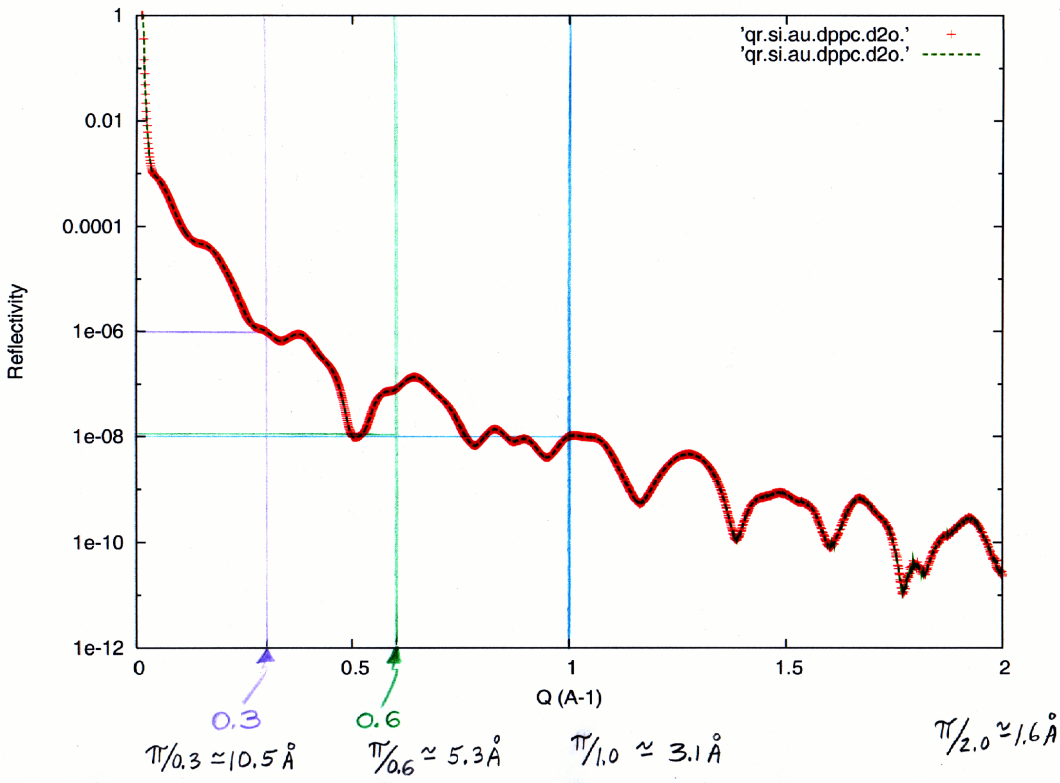
'qr.si.au.dppc.d2o.'
'qr.si.au.dppc.d2o.'
Reflectivity
Q (A-1)
0.3
0.6
π/0.3 ≃ 10.5 Å
π/0.6 ≃ 5.3 Å
π/1.0 ≃ 3.1 Å
π/2.0 ≃ 1.6 Å

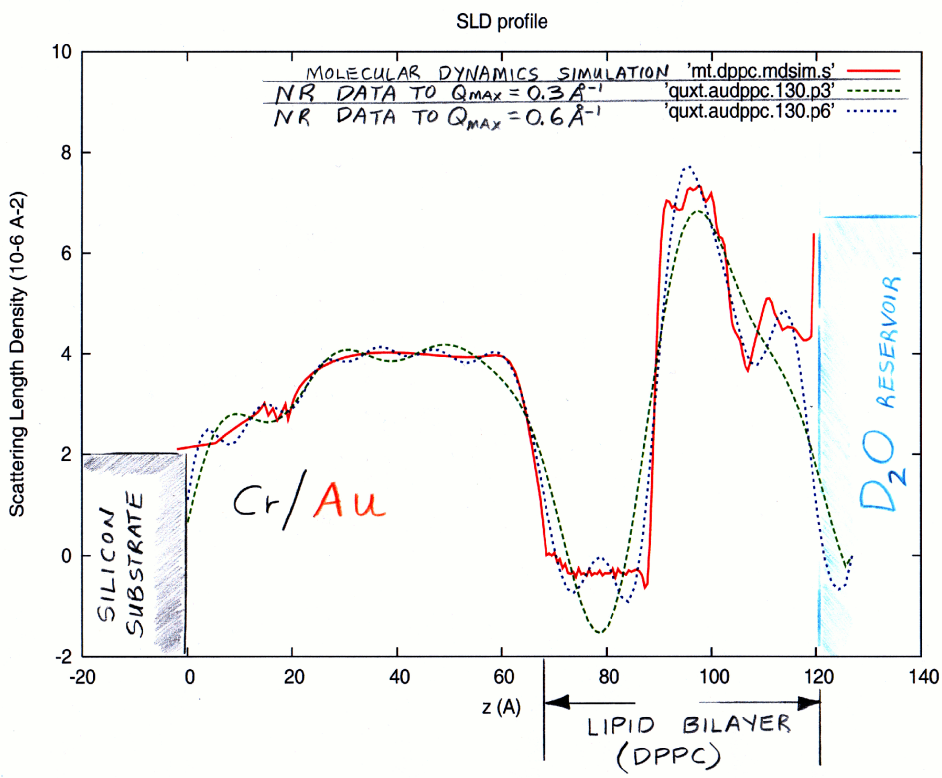
SLD profile
MOLECULAR DYNAMICS SIMULATION 'mt.dppc.mdsim.s'
NR DATA TO Q_MAX = 0.3 Å^-1 'quxt.audppc.130.p3'
NR DATA TO Q_MAX = 0.6 Å^-1 'quxt.audppc.130.p6'
Scattering Length Density (10-6 A-2)
z (A)
SILICON SUBSTRATE
Cr/Au
D2O RESERVOIR
LIPID BILAYER (DPPC)

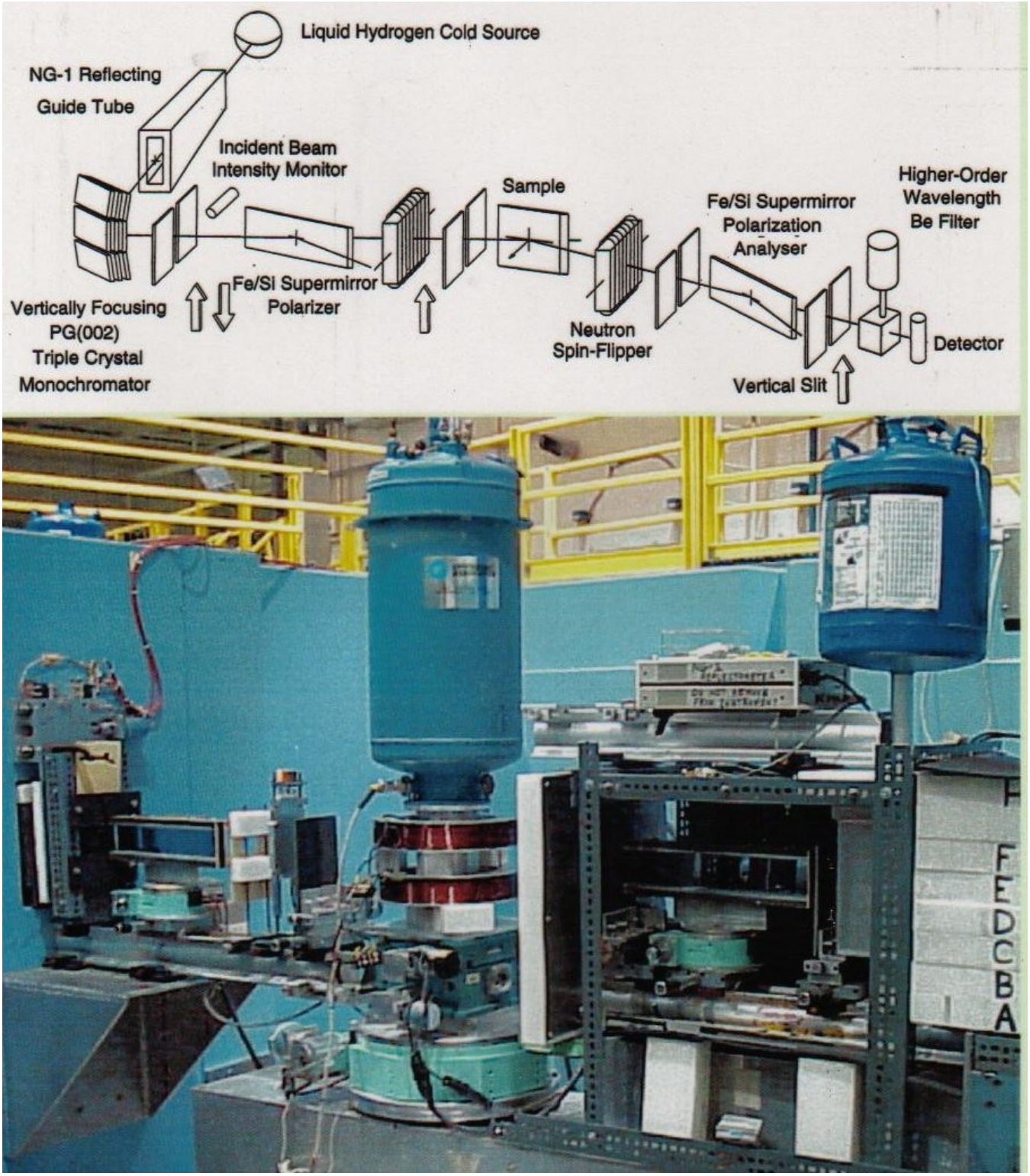

Polarized neutron reflectometer at NIST

Part 2: Applications of NR to studies of the nano-scale structure of thin film materials

<> Soft condensed matter:

-- polymers

-- bio-membranes

-- organic photo-voltaic films

. . .

<> Hard condensed matter:

-- magnetic materials (to be discussed in a following lecture)

-- chemical interdiffusion (e.g., 58Ni/62Ni)

-- metal hydrides

. . .

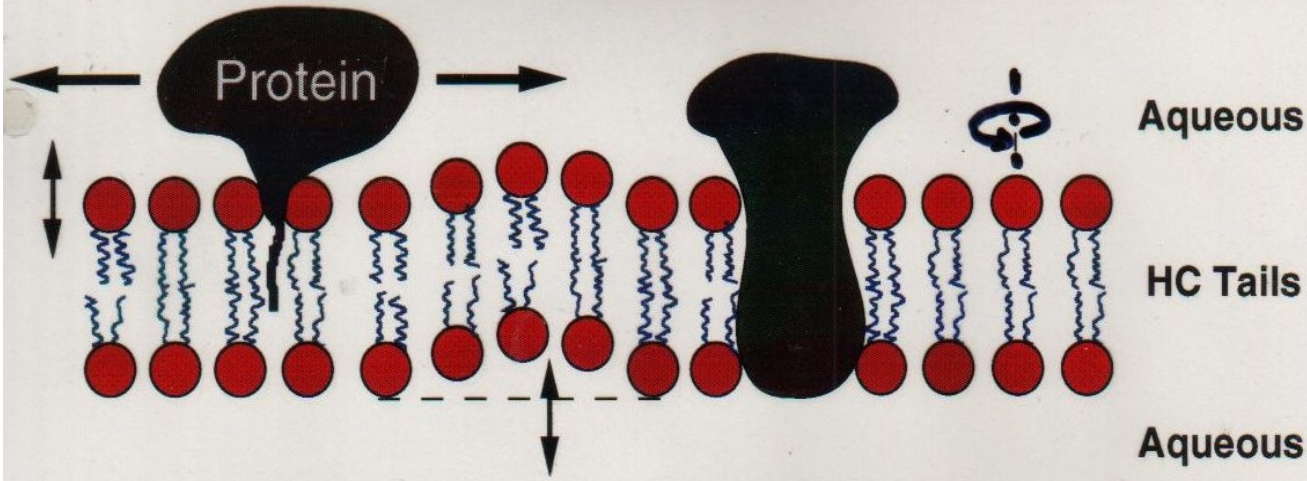

Supported Lipid Bilayers

A model system to mimic the structure and dynamics of cell membranes.

Proteins in Lipid Bilayers

- **Difficult to characterize by traditional x-ray crystallography.**
- **Play a crucial role in cell function**
  - **regulate ion and nutrient transport**
  - **engage in binding, signalling and cell recognition**
  - **participate in cell fusion events.**

Biosensors (Anne Plant & coworkers)

Melittin in Hybrid Bilayer Membranes

S. Krueger, A. Plant, et al., NIST
(Langmuir)

- pore-forming toxin
- used as model membrane peptide
- active in HBMs

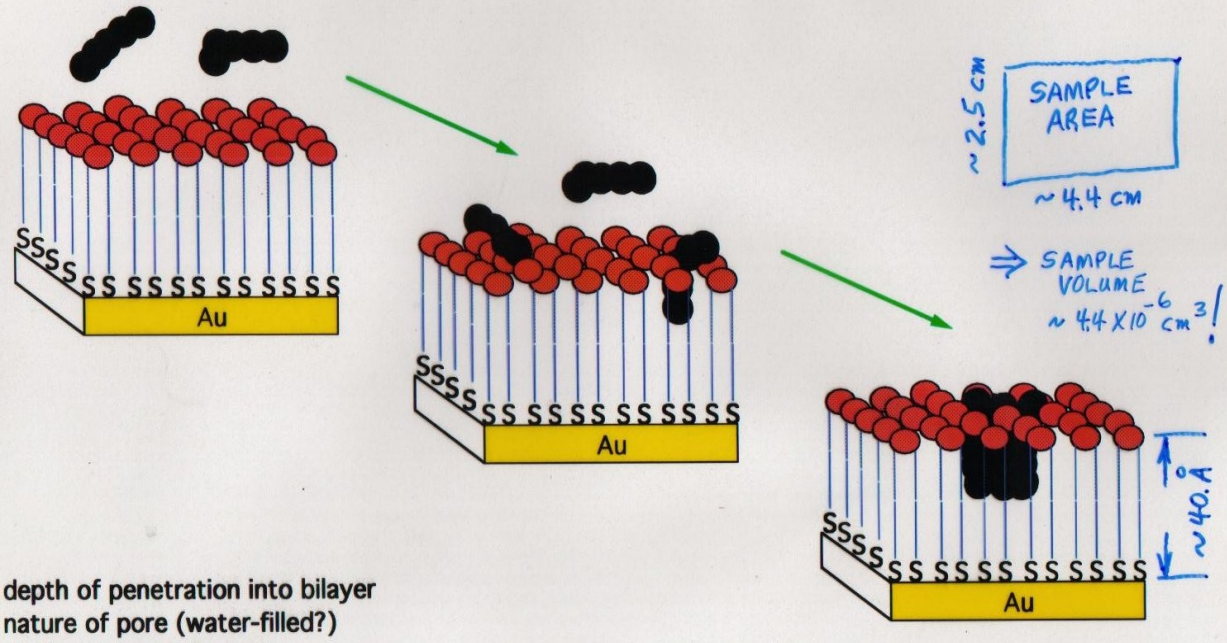

- depth of penetration into bilayer
- nature of pore (water-filled?)
- conformational changes
- random or ordered distribution?
- influence on surrounding lipids (location,conformation)

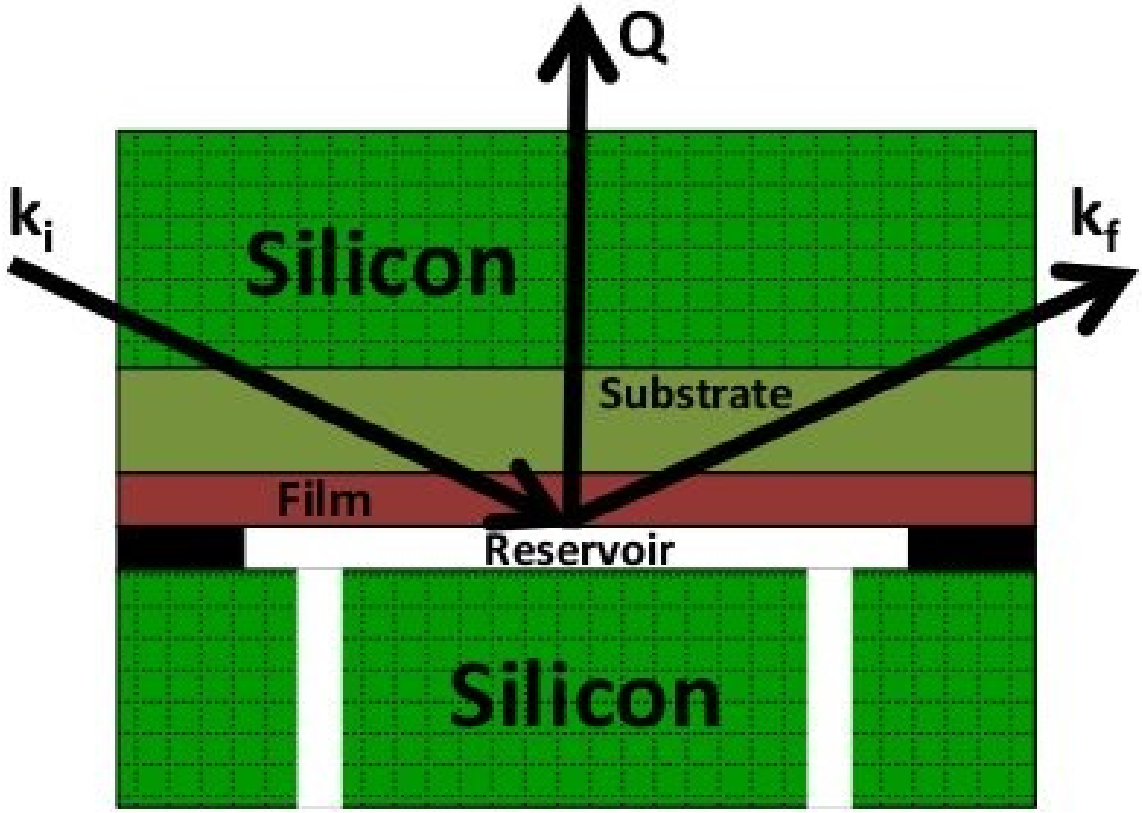
Q
k_i
k_f
Silicon
Substrate
Film
Reservoir
Silicon

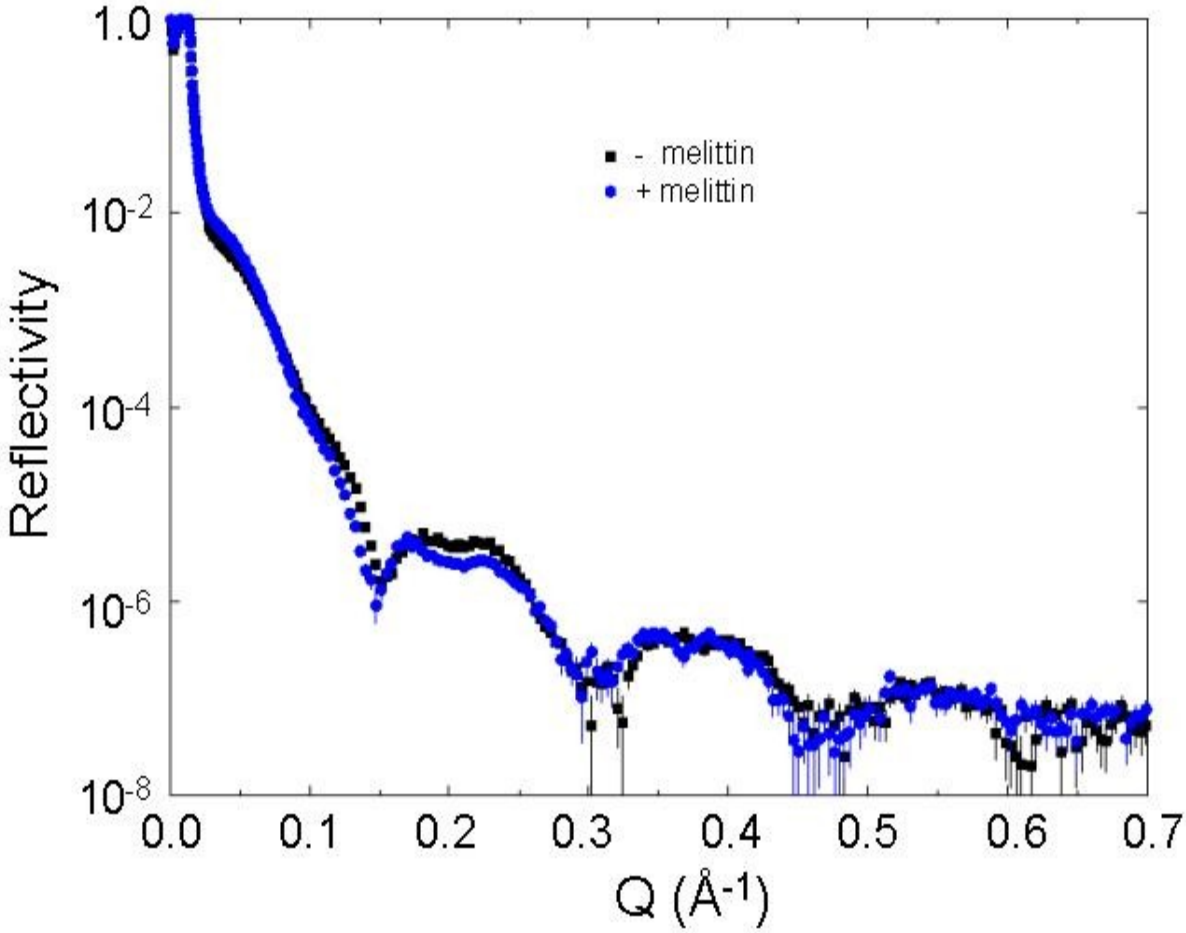
1.0
10-2
10-4
10-6
10-8
Reflectivity
- melittin
+ melittin
0.0
0.1
0.2
0.3
0.4
0.5
0.6
0.7
Q (Å-1)

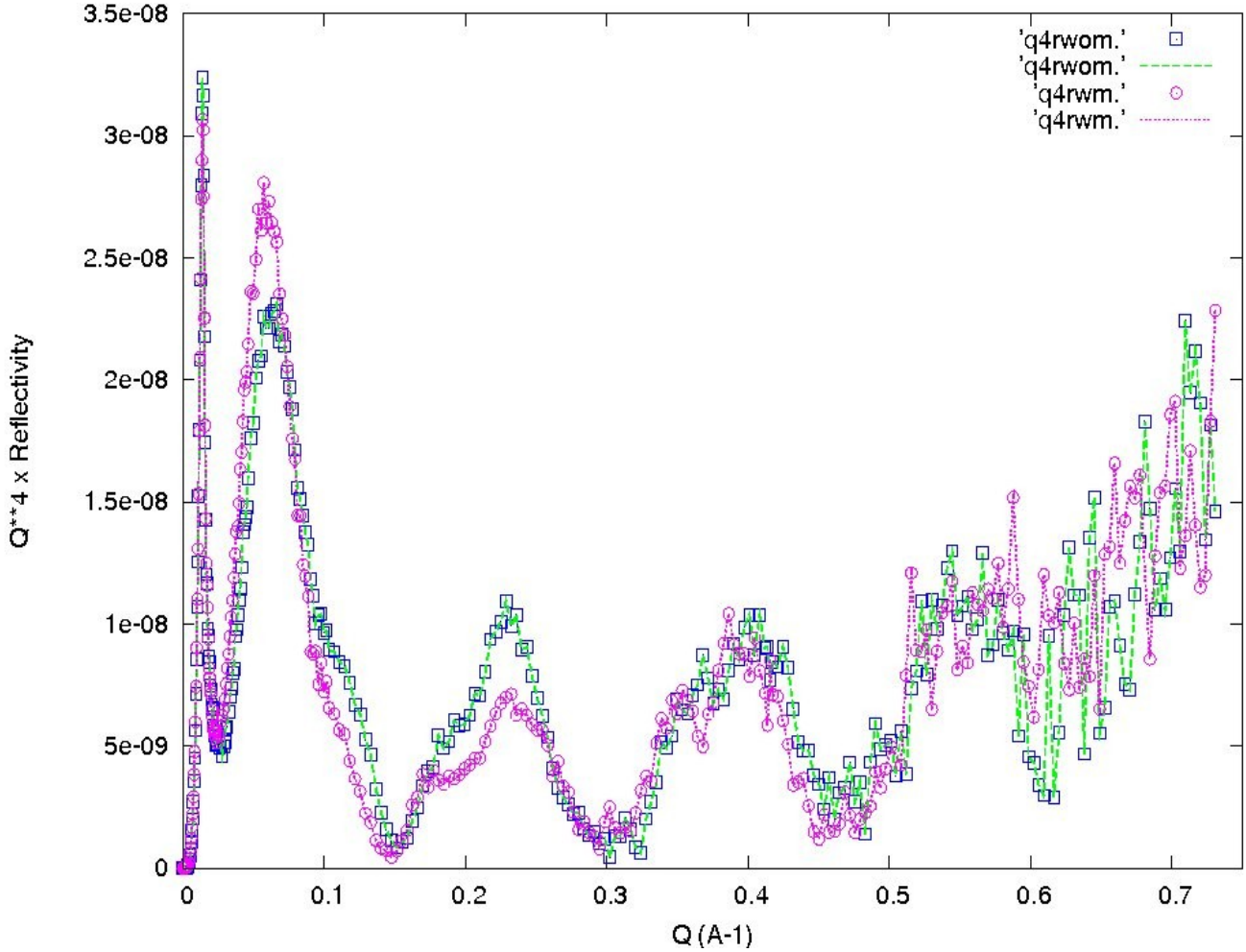
'q4rwom.'
'q4rwom.'
'q4rwm.'
'q4rwm.'
Q**4 x Reflectivity
Q (A-1)
3.5e-08
3e-08
2.5e-08
2e-08
1.5e-08
1e-08
5e-09
0
0
0.1
0.2
0.3
0.4
0.5
0.6
0.7

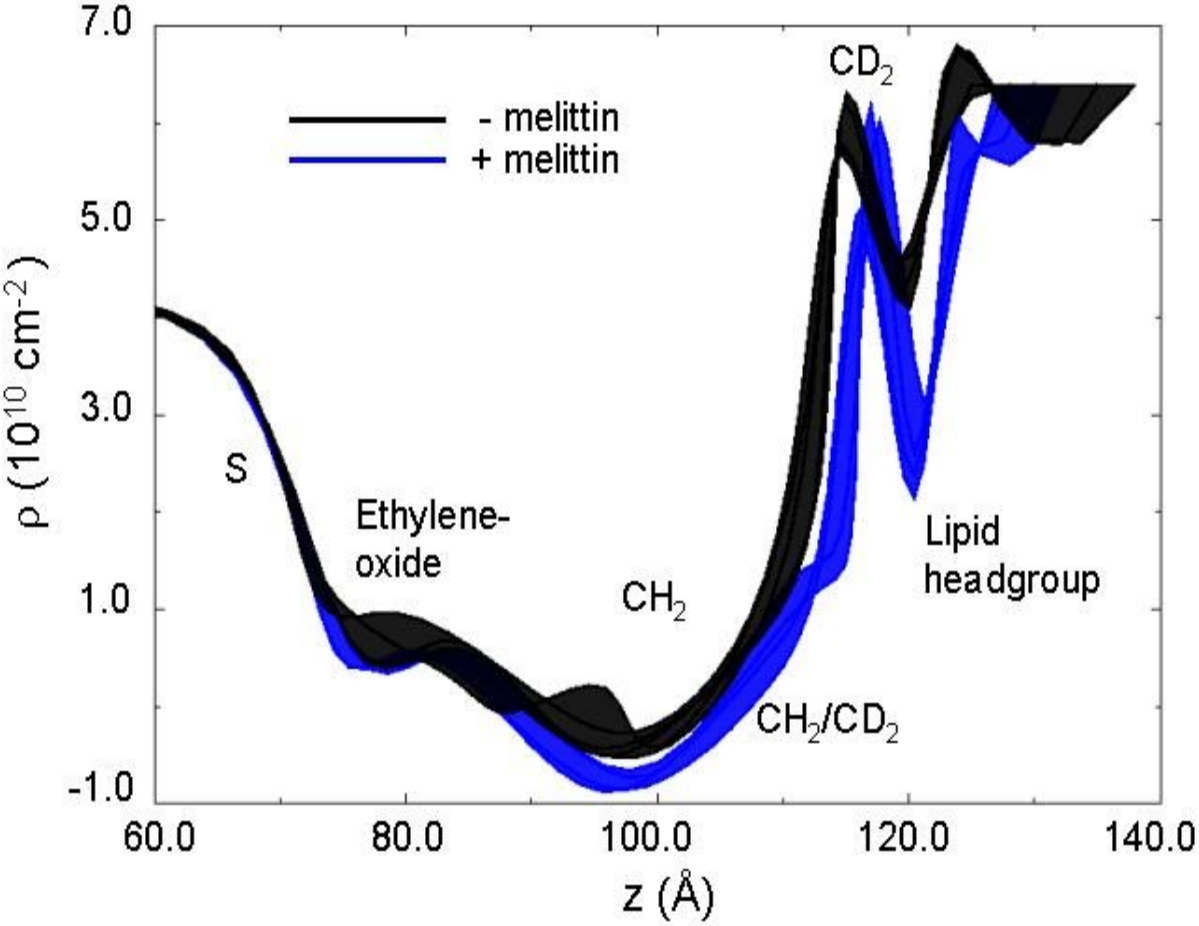
7.0
5.0
3.0
1.0
-1.0
ρ (10^10 cm^-2)
60.0
80.0
100.0
120.0
140.0
z (Å)
- melittin
+ melittin
CD2
S
Ethylene-
oxide
CH2
CH2/CD2
Lipid
headgroup

S. KRUEGER, C.F. MAJKRZAK, N.F. BERK, M. TAREK, D. TOBIAS, V. SILIN, J.A. DURA, C.W. MEUSE, J. WOODWARD, A.L. PLANT

(Langmuir)

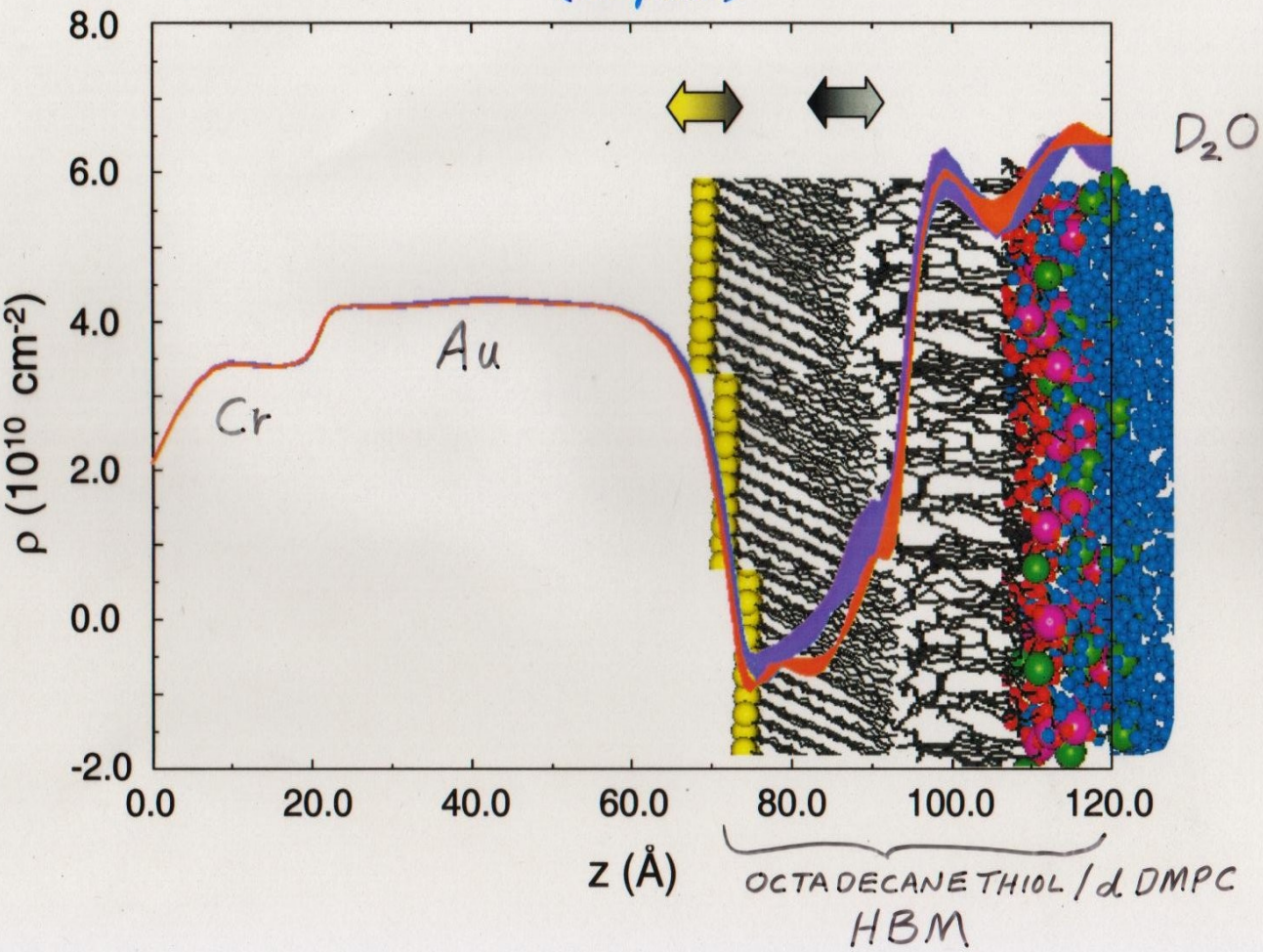

Water-soluble membrane-associated proteins

>50% of biological NR beam time for biomedical applications using tBLMs

Active projects (last 2 cycles):

- Dengue
- Gaucher's disease
- GRASP
- HIV Gag & antibodies
- RSV & MLV
- Neurotransmitter
- OmpA/LA
- Parkinson's disease
- PTEN Tumor surpressor
- T-Cell receptor

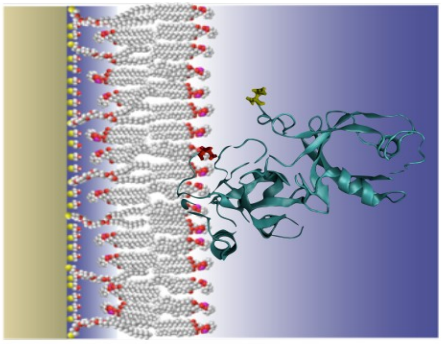

GRASP orientation at a tethered bilayer lipid membrane (tBLM) as determined by NR

Collaborative staff involvement:

- experimental planning
- substrate preparation
- tether synthesis
- neutron measurement
- data analysis

Bulent Akgun, Frank Heinrich, Mathias Lösche, Duncan McGillivray, Hirsh Nanda, David Vanderah

Typical reflectometry data for tBLM experiments

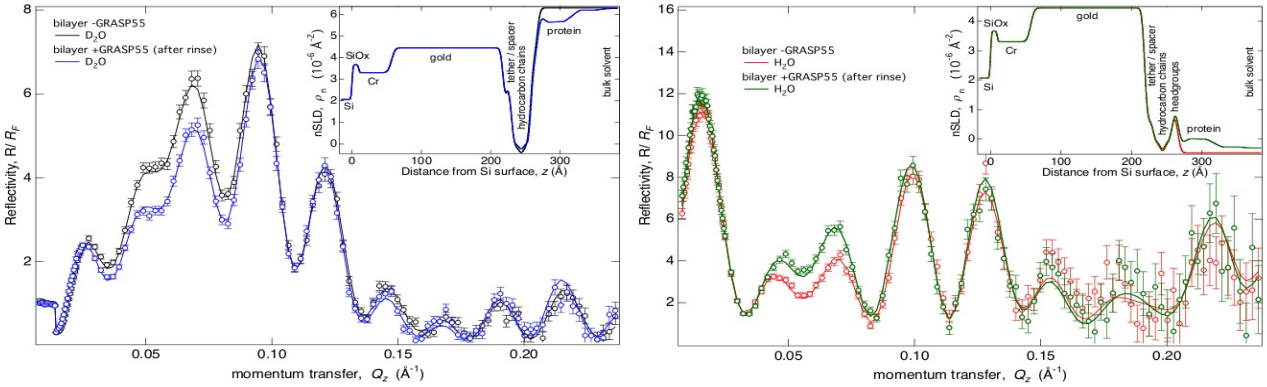

NR data measured on NG7, and best-fits for GRASP association with lipid membranes, project with A. Linstedt, University of Pittsburgh

Bulent Akgun, Frank Heinrich, Mathias Lösche, Duncan McGillivray, Hirsh Nanda

Example: Dengue Virus Envelope Protein

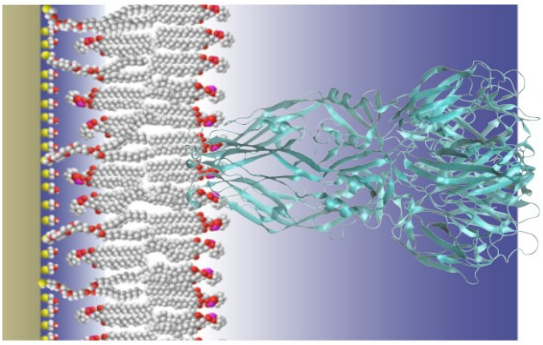

Visualization. Project with Mike Kent, Sandia National Labs.

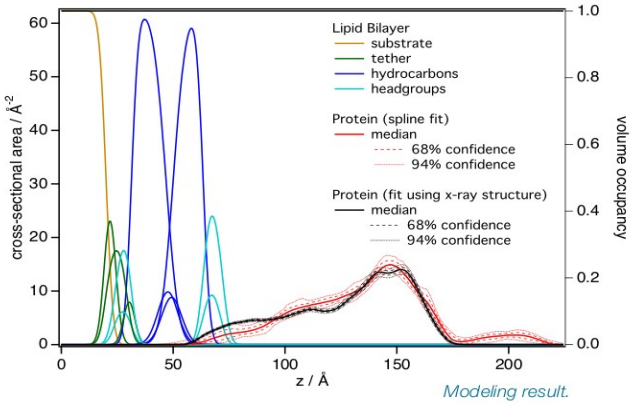

Modeling result.

- Monte-Carlo Markov Chain uncertainty analysis
- Composition-space modeling of the bilayer
- Free-form fitting of structurally unknown components of the architecture
- Usage of PDB structure files for position and orientation of rigid proteins

Bulent Akgun, Frank Heinrich, Paul Kienzle, Sushil Satija

www.ncnr.nist.gov/programs/reflect/

Combining NR with Molecular Simulations

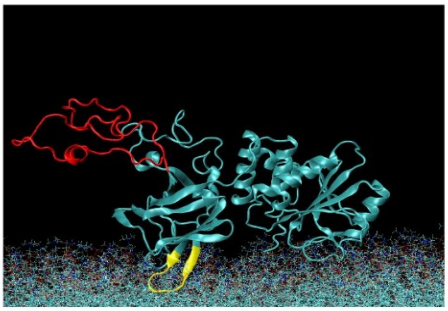

MD simulation snapshot of PTEN tumor suppressor association with a PS-containing lipid membrane

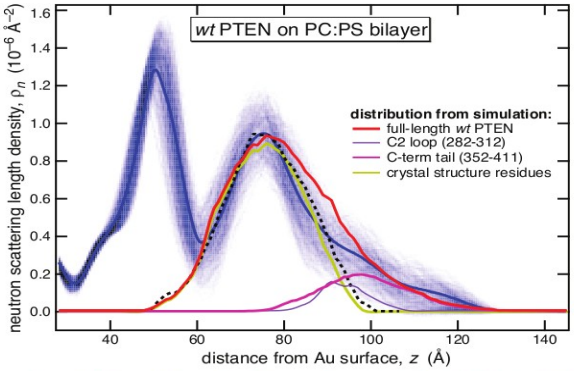

Comparison of MD and NR results, Shenoy, S. et al.. J. Struct. Biol. 1–15 (2012).

Comparison of experimental data with results from:
- MD simulation
- Monte Carlo conformational search (SASSIE) results

Future Challenges:
- Ensemble averaging, integrating NR and simulation

Joseph Curtis, Mathias Lösche, Hirsh Nanda

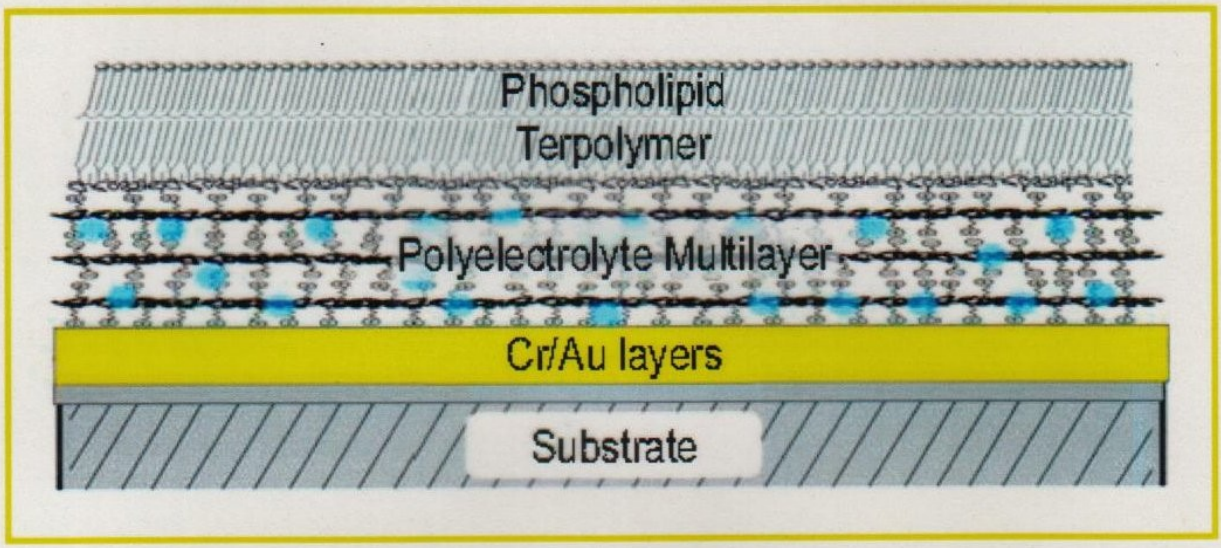

Fig. 1. Schematic diagram of a biomimetic membrane. The phospholipid layer at the top combines with the terpolymer layer to form a membrane-mimic that in turn resides on the water (blue dots) permeable "cushion" polyelectrolyte multilayer. The latter attaches electrostatically to the Au-capped substrate.

(Work of Ursula Perez-Salas, K. Faucher, E. Chaikof, et al.)

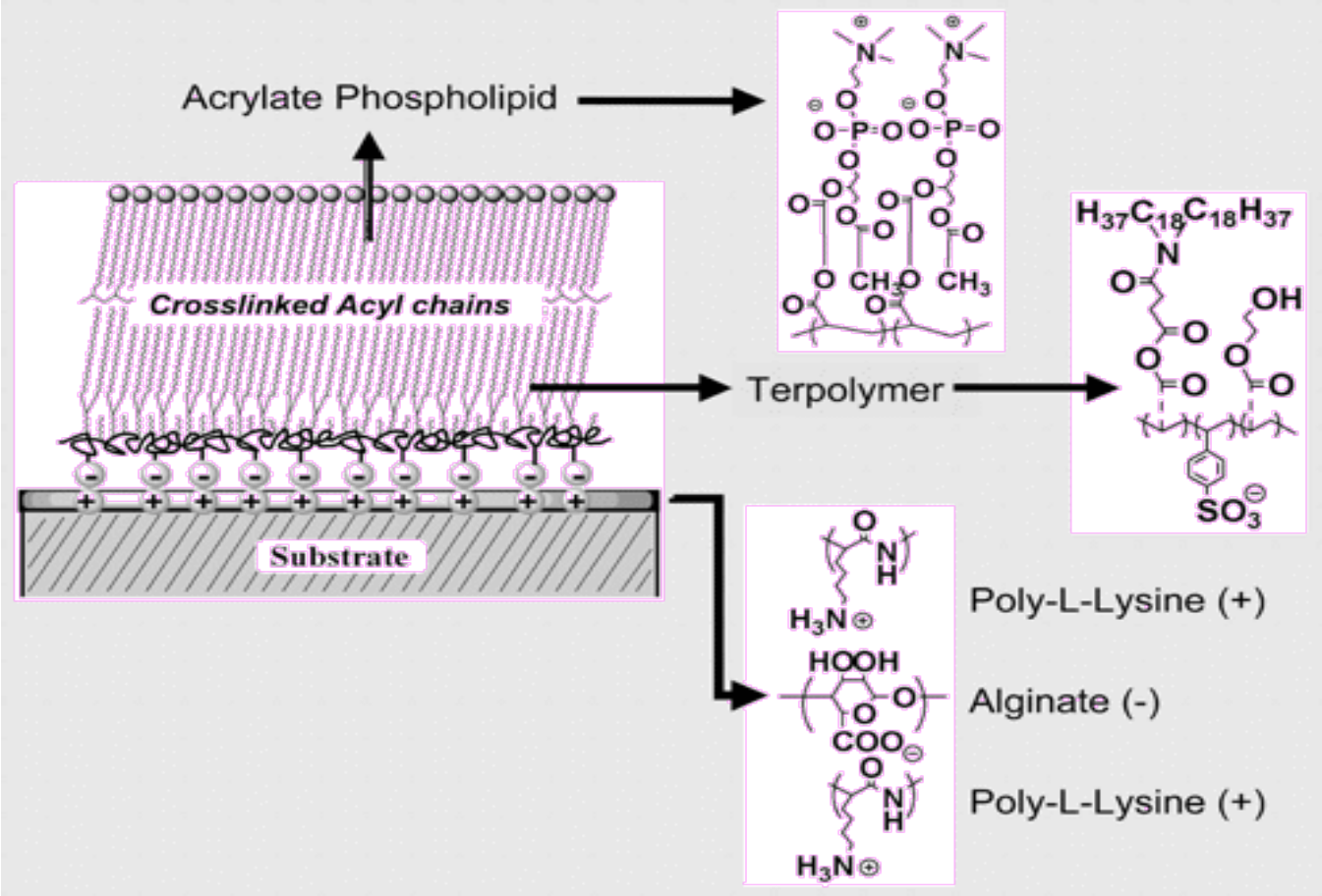
Acrylate Phospholipid
Crosslinked Acyl chains
Substrate
Terpolymer
Poly-L-Lysine (+)
Alginate (-)
Poly-L-Lysine (+)

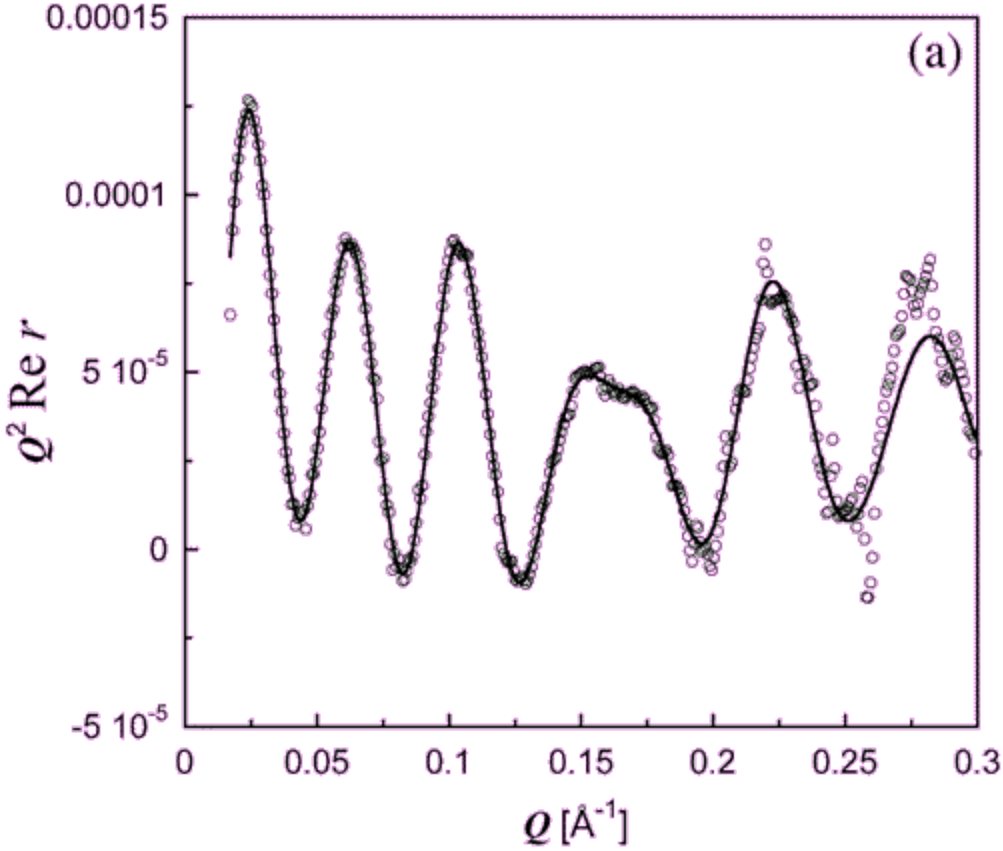
(a)
0.00015
0.0001
5 10^-5
0
-5 10^-5
Q^2 Re r
0
0.05
0.1
0.15
0.2
0.25
0.3
Q [Å^-1]

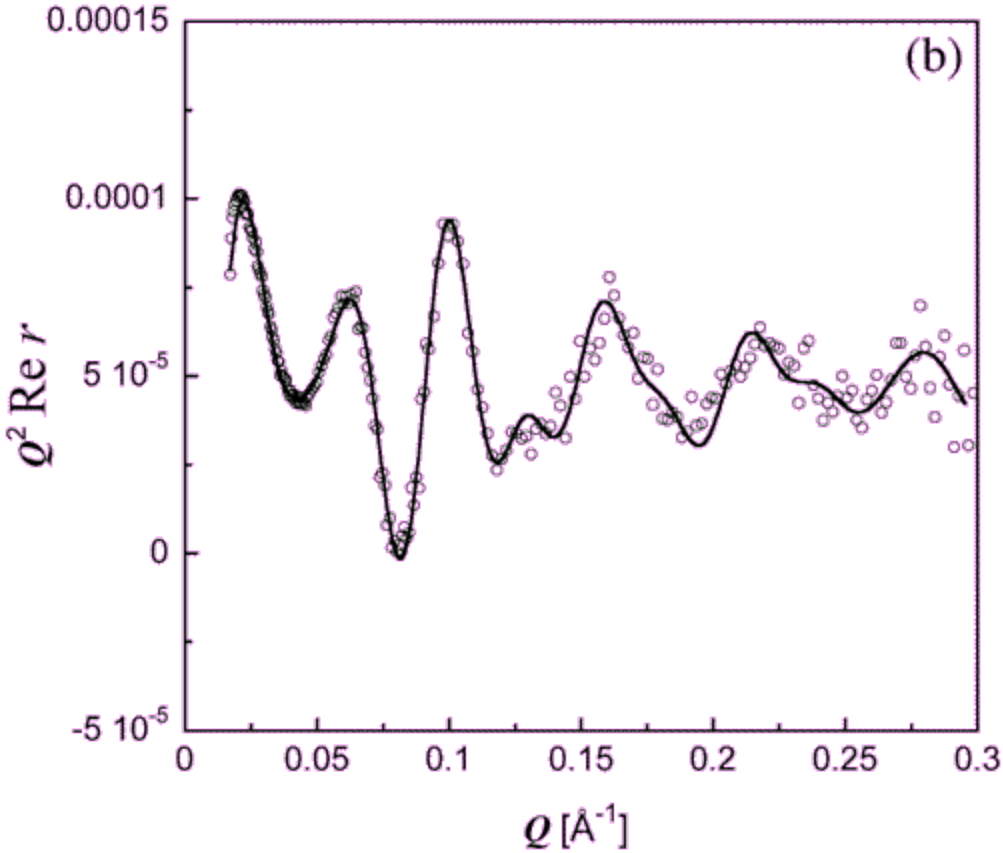
(b)
0.00015
0.0001
5 10^-5
0
-5 10^-5
Q^2 Re r
0
0.05
0.1
0.15
0.2
0.25
0.3
Q [Å^-1]

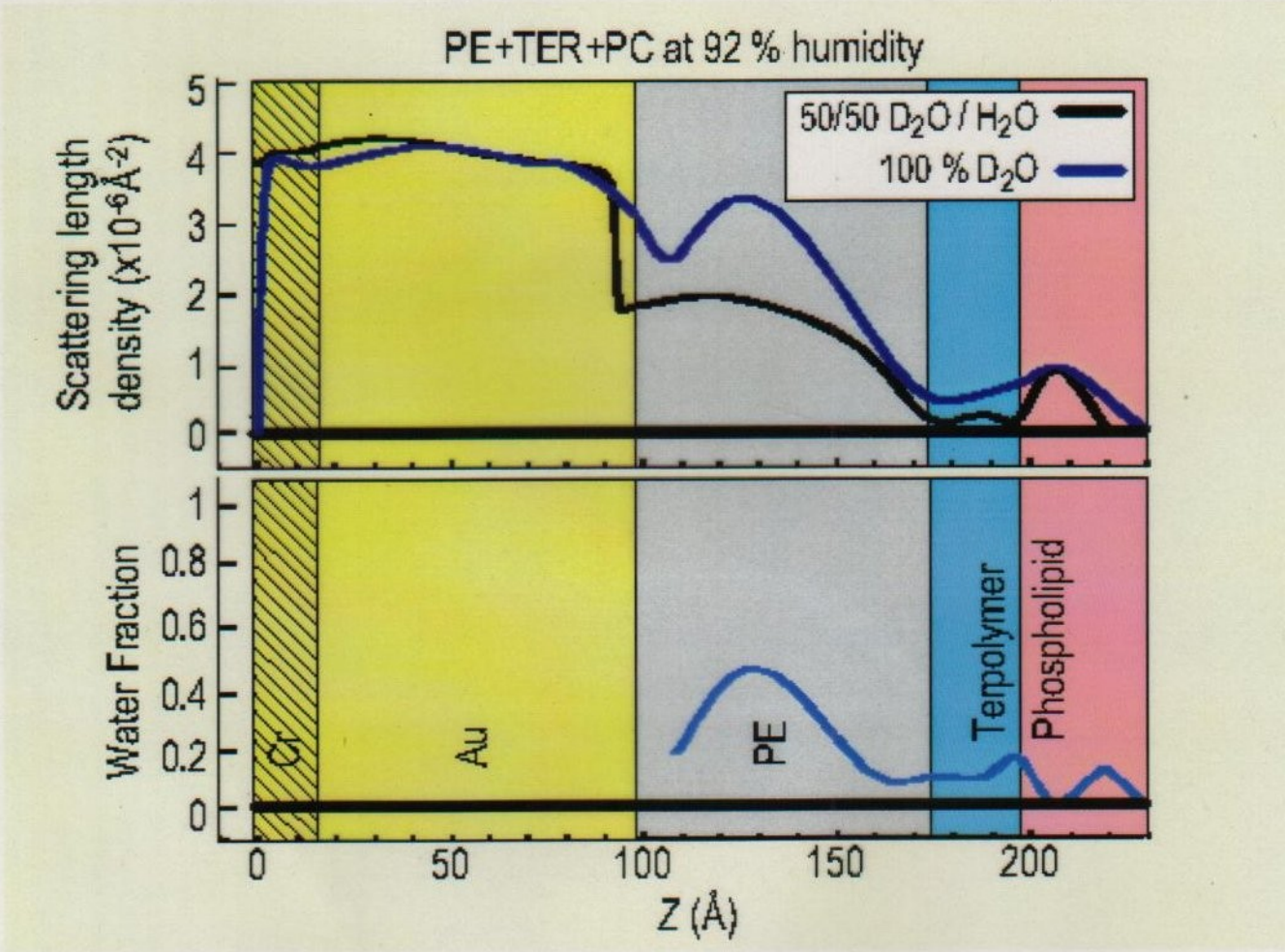

Fig. 3. Scattering length density profiles (top) and water fraction (bottom) for PE+TER+PC under indicated conditions.

Nanoparticle distribution in polymer-based solar cells affects solar cell performance: A neutron reflectivity study

Jonathan Kiel[1], Brian Kirby[2], Charles Majkrzak[2],
Brian Maranville[2], Michael Mackay[3]

Thursday, August 20th, 2009

1) Michigan State University, Department of Chemical Engineering and Materials Science
2) National Institute of Standards and Technology, Center for Neutron Research
3) University of Delaware, Materials Science and Engineering

UNIVERSITY OF DELAWARE

MICHIGAN STATE UNIVERSITY

NIST Center for Neutron Research

Components of organic solar cells

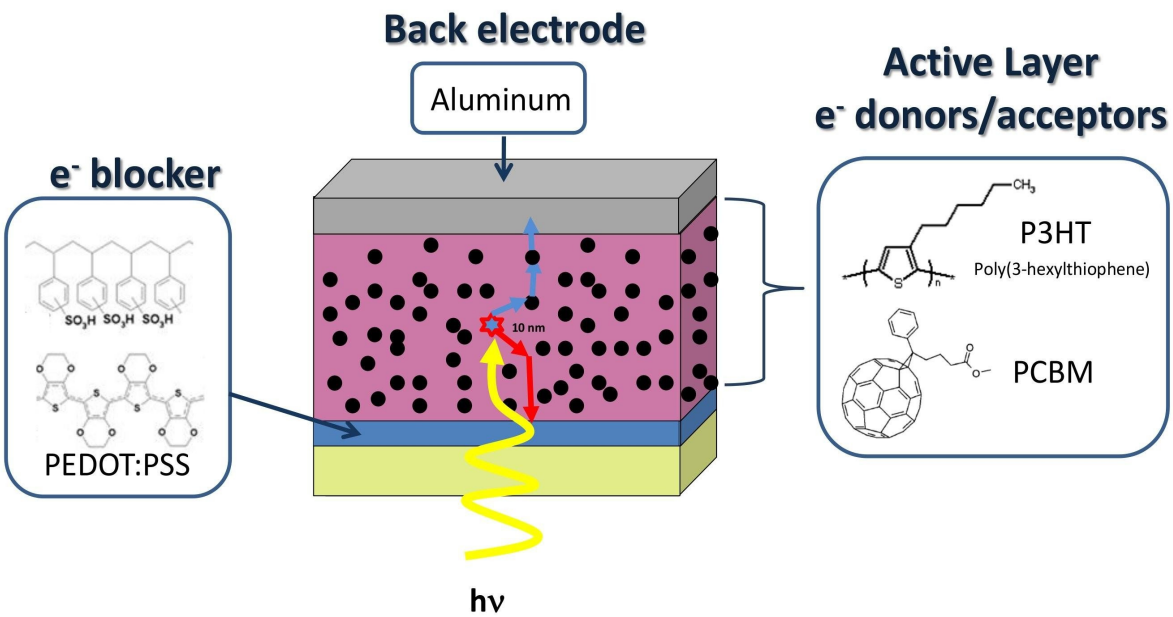

- Exciton diffusion length ~10 nm
- PCBM:P3HT morphology very important

What is the morphology of the active layer

Energy Diagram of Organic Solar Cell

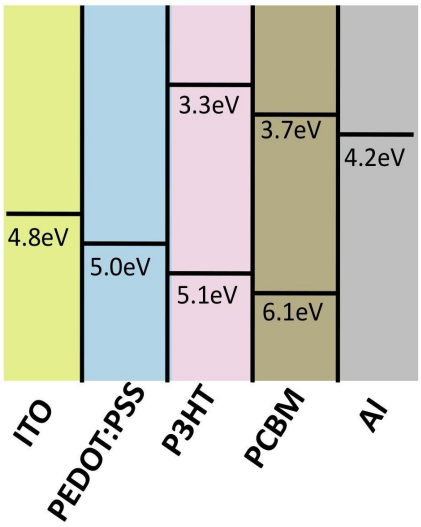

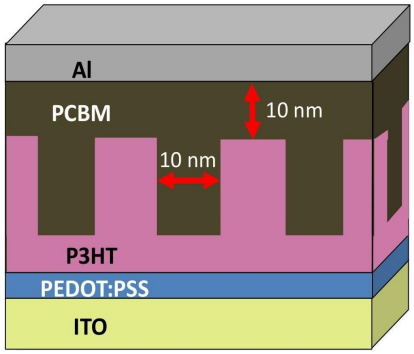

Idealized morphology

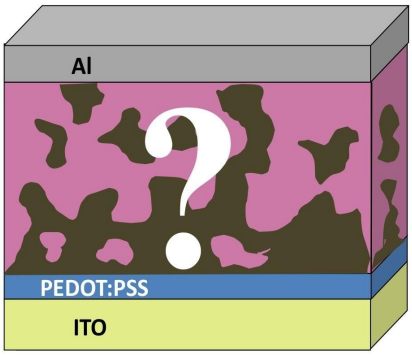

Actual morphology

K. M. Coakley, M. D. McGehee, *Chemical Materials,* **2004**

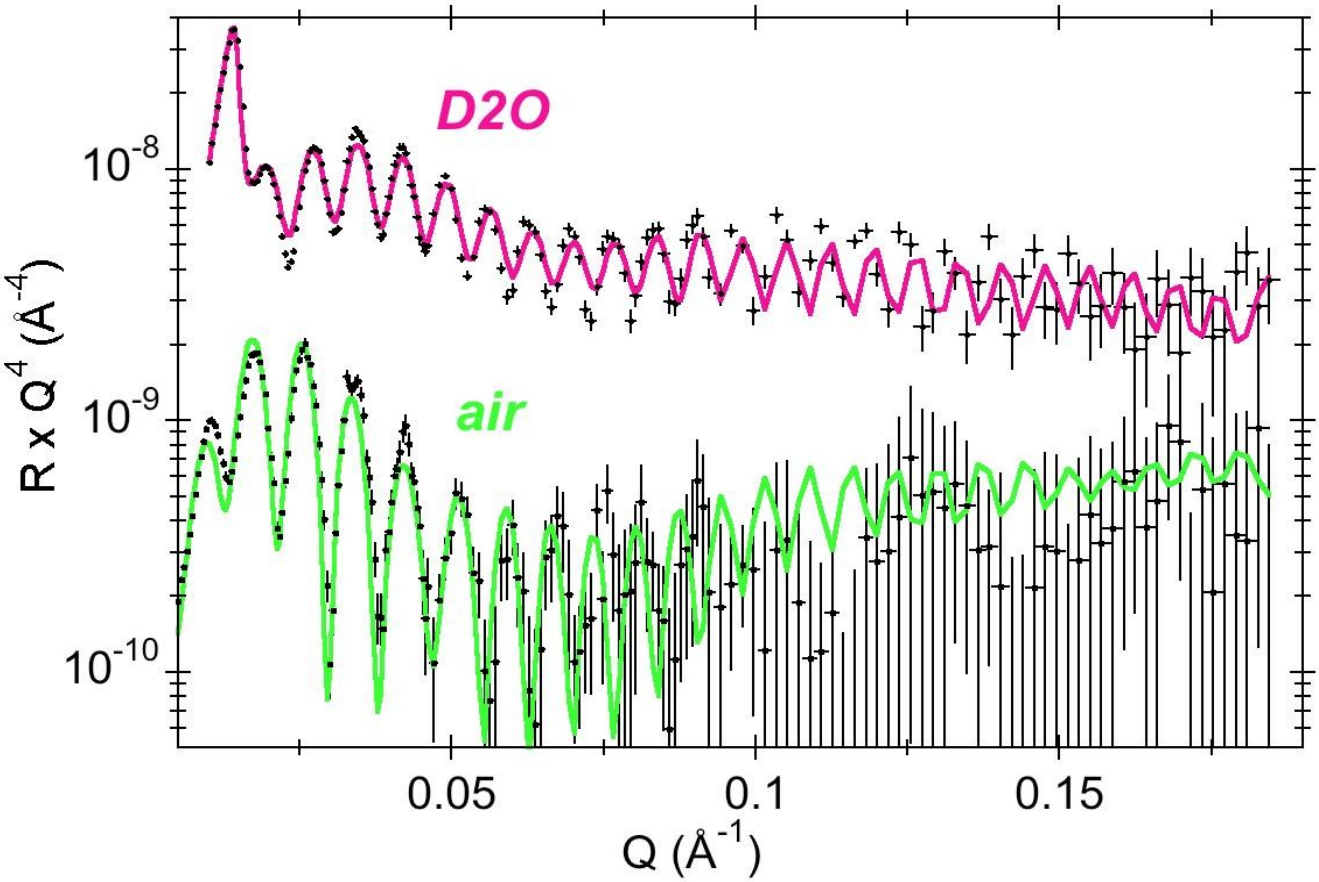
D2O
air
10^{-8}
10^{-9}
10^{-10}
R x Q^4 ($Å^{-4}$)
0.05
0.1
0.15
Q ($Å^{-1}$)

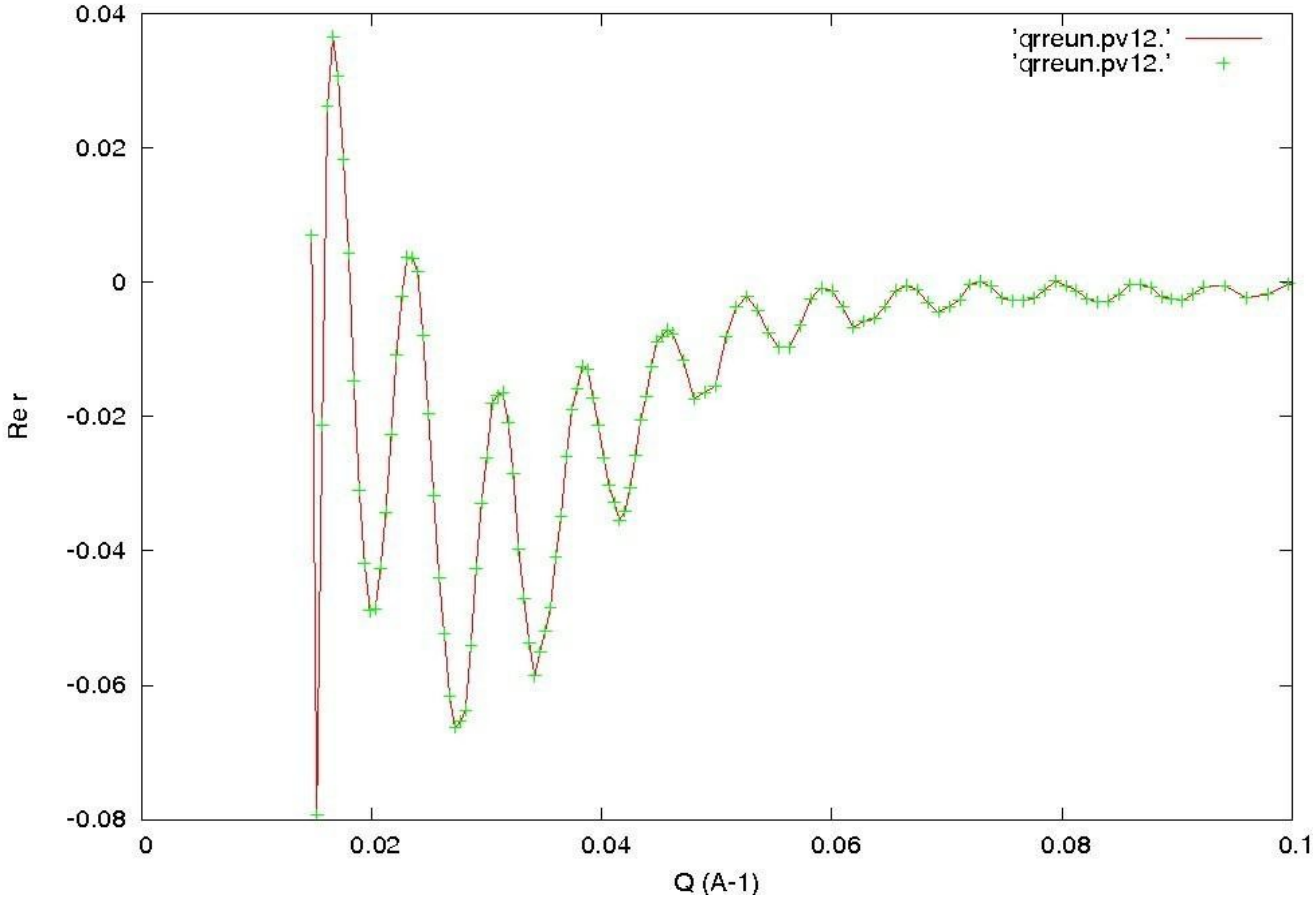
'qrreun.pv12.'
'qrreun.pv12.'
Re r
Q (A-1)
0.04
0.02
0
-0.02
-0.04
-0.06
-0.08
0
0.02
0.04
0.06
0.08
0.1

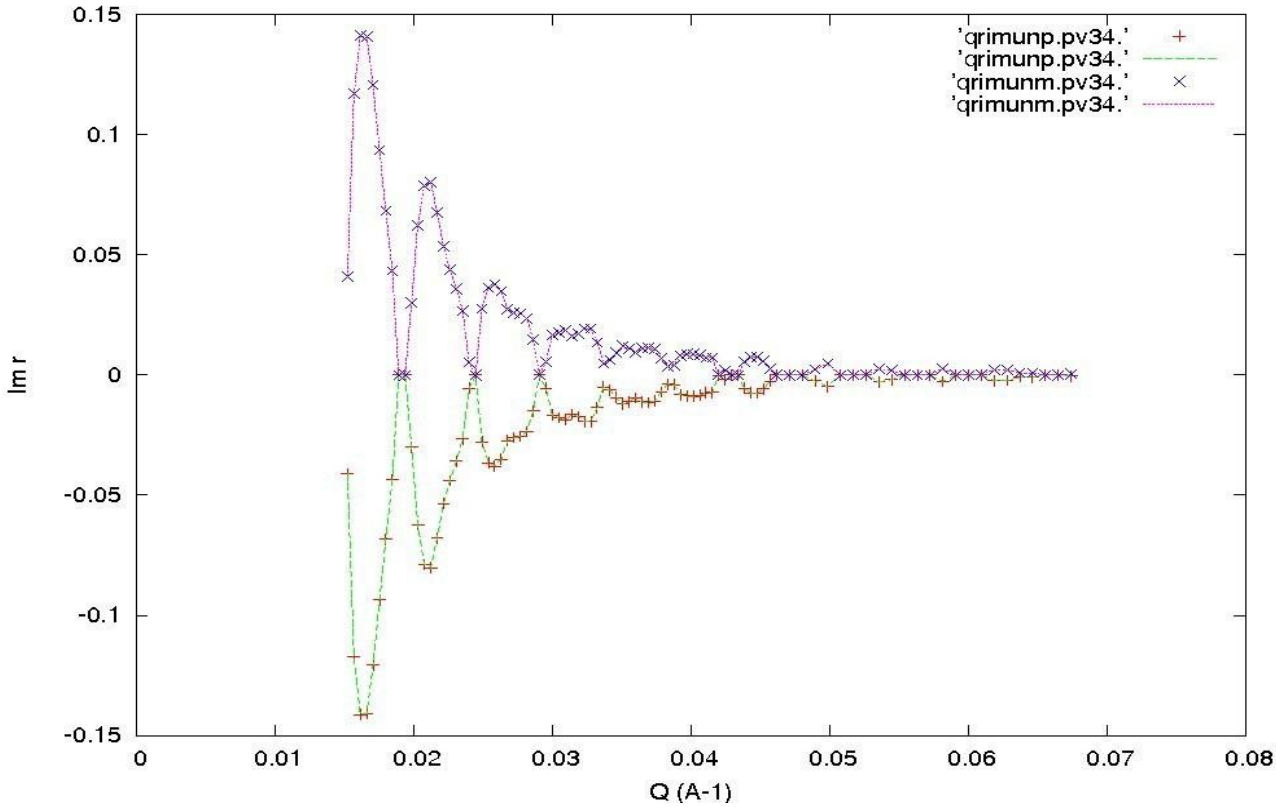
'qrimunp.pv34.'
'qrimunp.pv34.'
'qrimunm.pv34.'
'qrimunm.pv34.'
Im r
Q (A-1)
0.15
0.1
0.05
0
-0.05
-0.1
-0.15
0
0.01
0.02
0.03
0.04
0.05
0.06
0.07
0.08

PCBM Volume % Comparison

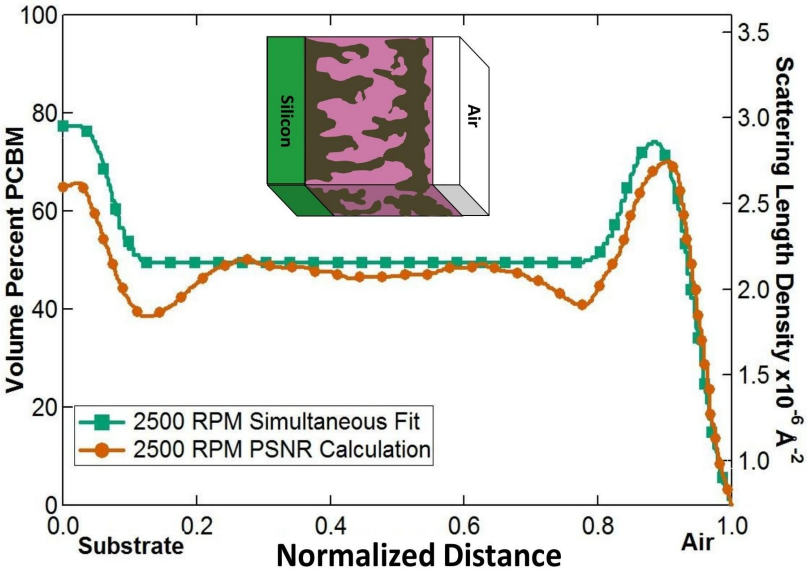

$$\text{Vol\% PCBM} = \frac{SLD_{measured} - SLD_{P3HT}}{SLD_{PCBM} - SLD_{P3HT}}$$

- Simultaneous fitting and PSNR calculations show great agreement
- High PCBM concentration at substrate
- High PCBM concentration near air interface

Diblock copolymer lamellar nanostructures – R.Jones, B.Berry, and K.Yager (NIST Polymer Division) and S.Satija, J.Dura, B.Maranville et al. (NCNR).

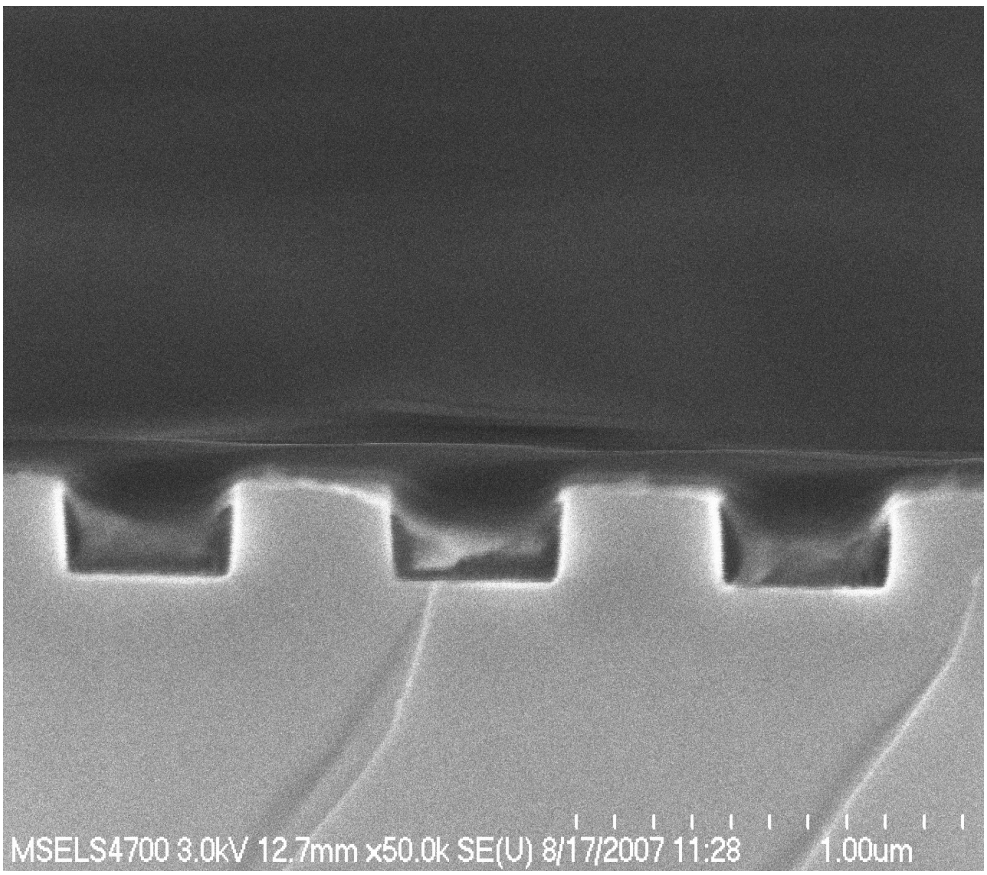

Side-view scanning-electron micrograph of laser-interferometry-produced silicon substrate with 400 nm channels, spaced by 400 nm for a total repeat distance of 800 nm.

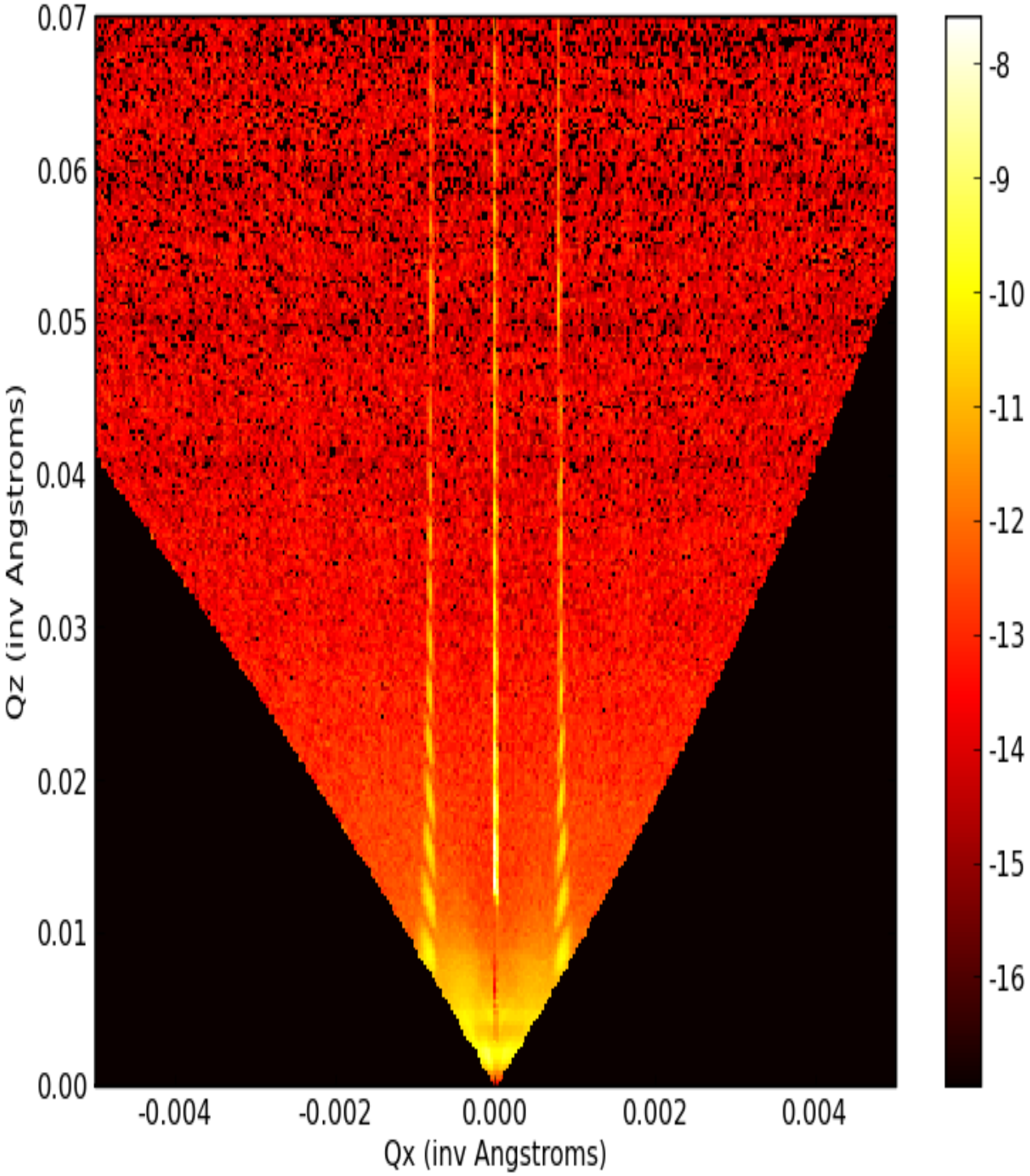

Neutron diffraction from silicon with channels but without polymer.

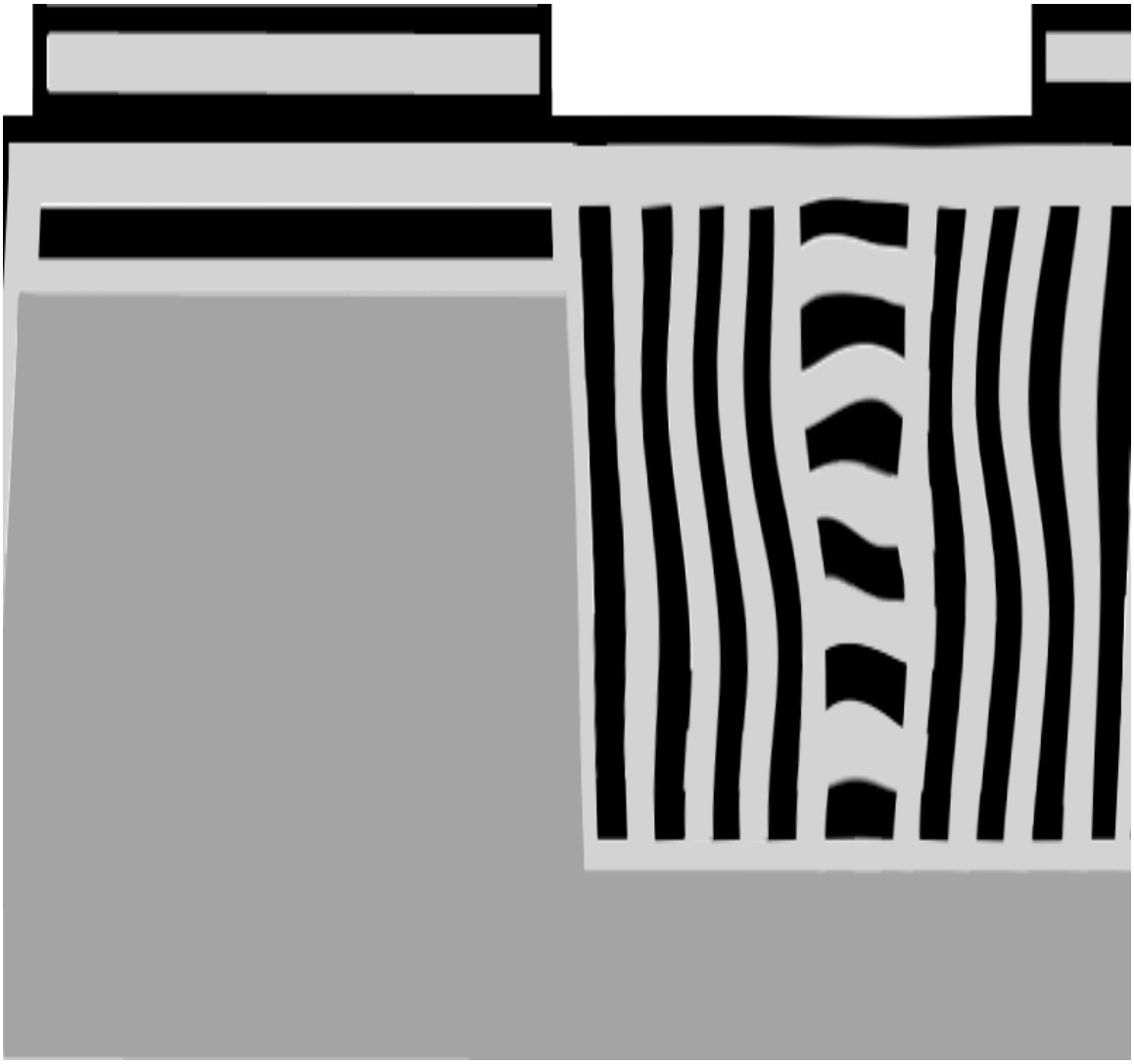

Diagram of expected orientation of lamellae, based on position with respect to the channels. Silicon substrate with etched channels is displayed in gray, with lighter and darker regions corresponding to the two polymer components of the lamellae.

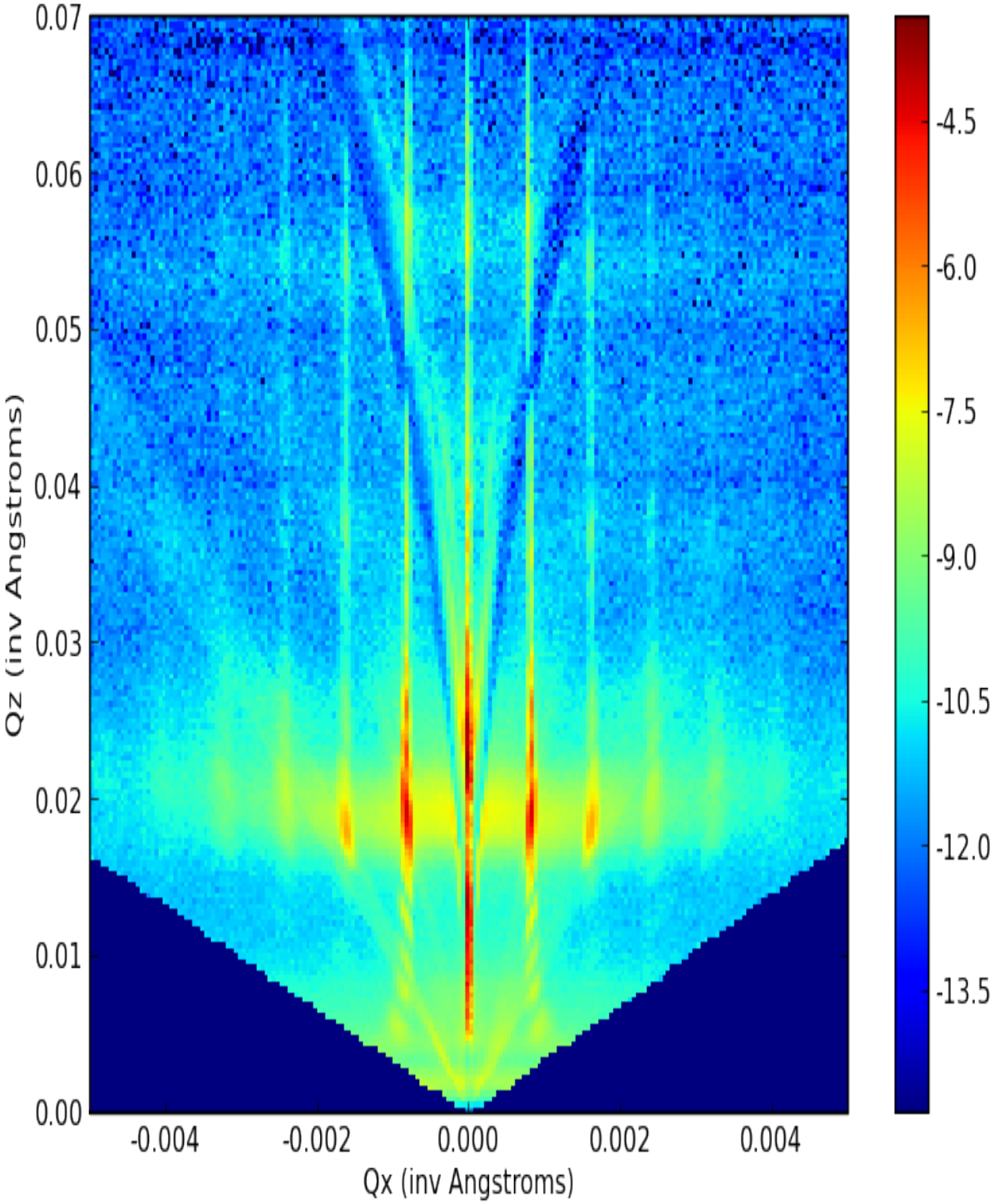

Neutron diffraction from Si channels filled with ordered diblock copolymer.

Part 3: The Phase problem, Direct Inversion and Simultaneous Fitting

<> ambiguous SLD profiles from reflected *intensities*

<> measurement of reflection *amplitude* via references yields unique solution -- one-to-one correspondence with SLD profile

<> given the reflection amplitude, exact, first-principles inversion to obtain unique SLD profile for specular reflection is possible

<> simultaneous fitting of multiple composite (sample + reference) reflectivity data sets can lead to unambiguous solution as well

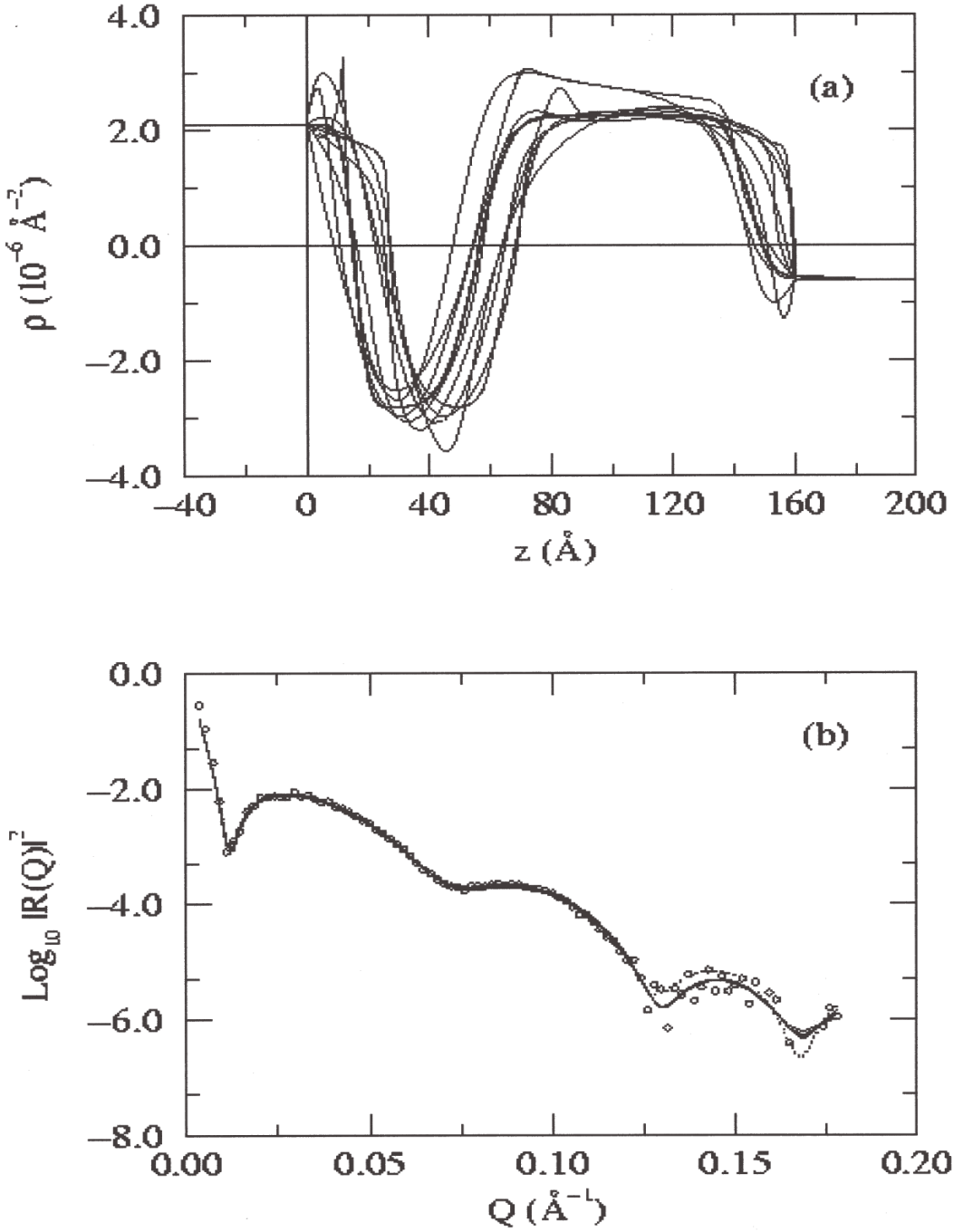

Repeated fits of reflectivity data from a Ti/TiO film system on a Si substrate in contact with an aqueous reservoir (Berk et al.).

PBS

TiO in situ: Wiesler, et al.

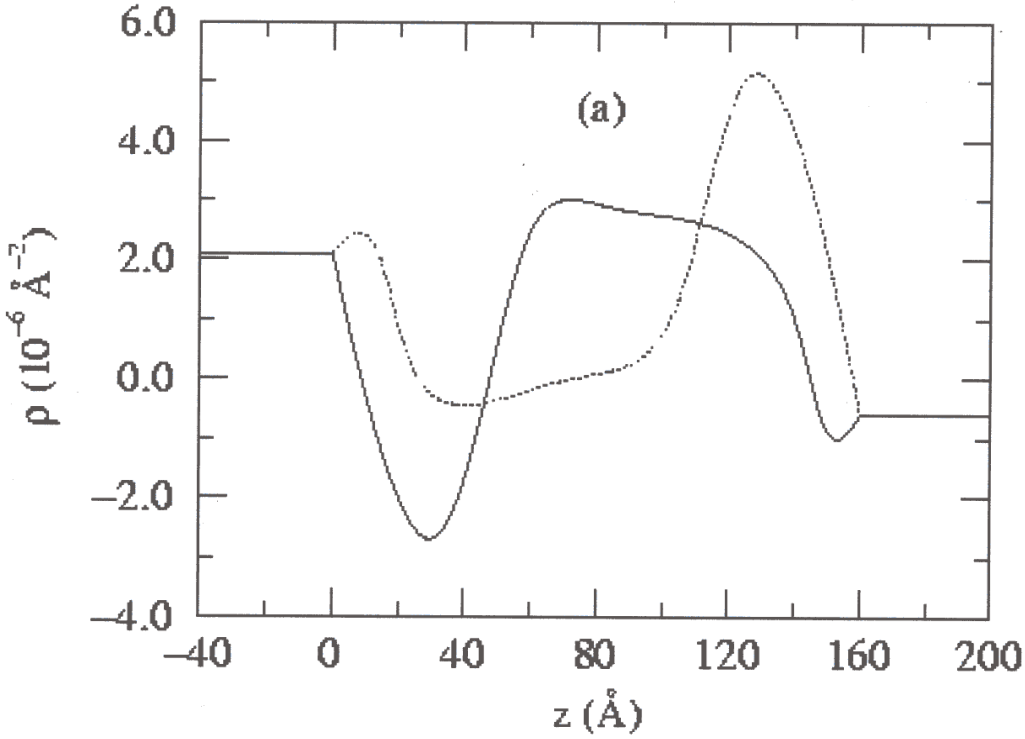

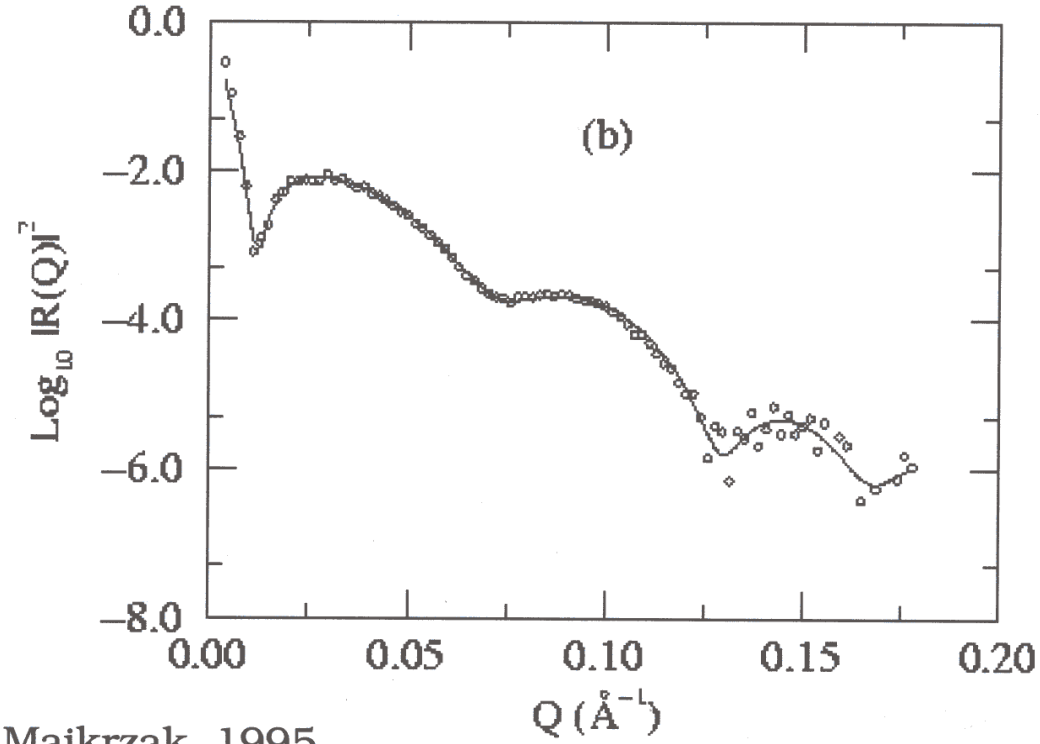

Berk & Majkrzak, 1995

Inverting reflectivity

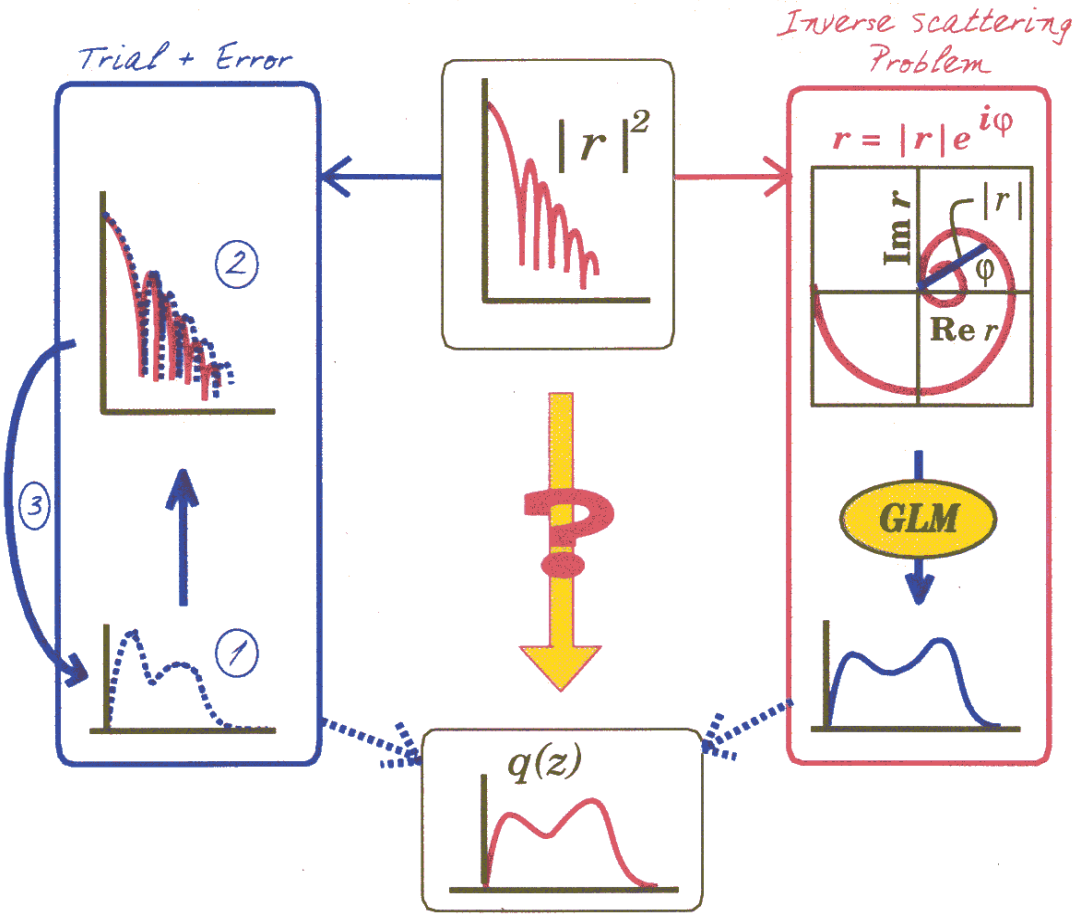

Phase determination
C.F. Majkrzak and N.F. Berk, Phys. Rev. B **52**, 10827 (1995).
V.–O. de Haan, et al., Phys. Rev. B **52**, 10830 (1995).

H. Leeb, H.R. Lipperheide and G. Reiss, this conference.

Logarithmic dispersion
W.L. Clinton, Phys. Rev. B **48**, 1 (1993).
Tunneling times
H. Fiedeldey, H.R. Lipperheide, et al., Phys. Lett. A **170**, 347 (1992).

Pseudo–inversion
S.K. Sinha, et al., *Surface X–Ray and Neutron Scattering*, 85 (Springer, 1992).
C.F. Majkrzak, N.F. Berk, et al., SPIE Proc. **1738**, 282 (1992).

NIST

Phase Determination with 3 References

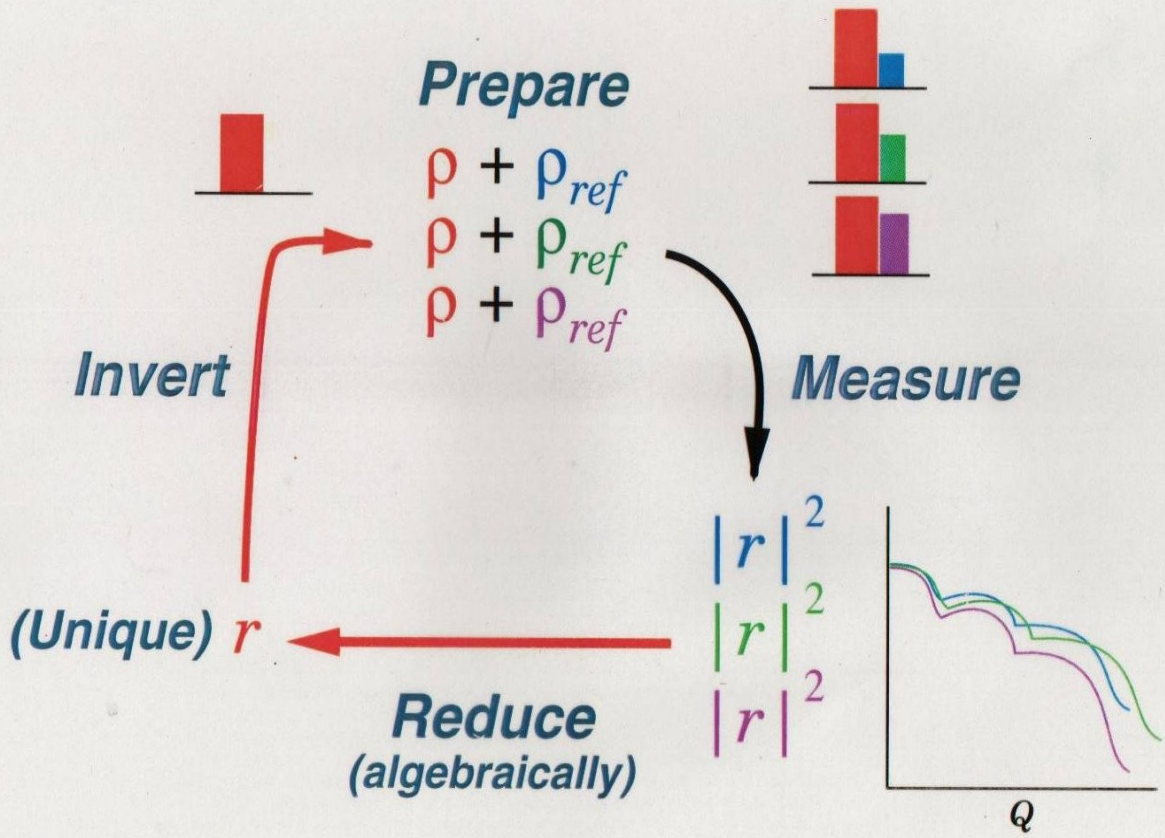

Majkrzak & Berk, 1995
de Haan, et al., 1995

FORMALISM ALLOWS A COMPOSITE POTENTIAL TO BE EXPRESSED AS A PRODUCT:

$$\underbrace{\begin{pmatrix} A & B \\ C & D \end{pmatrix}}_{\substack{\text{COMPOSITE} \\ (1,2,3)}} = \underbrace{\begin{pmatrix} a & b \\ c & d \end{pmatrix}}_{\text{UNKNOWN}} \underbrace{\begin{pmatrix} w & x \\ y & z \end{pmatrix}}_{\text{REFERENCE}}$$

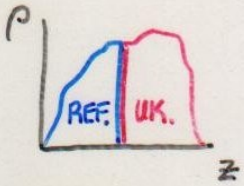

(1, 2, 3)

$$|R(Q)|^2 = |R_1(Q)|^2,\ |R_2(Q)|^2, \text{ and } |R_3(Q)|^2$$

$$\Sigma_i \equiv 2\left[\frac{1+|R_i|^2}{1-|R_i|^2}\right] = A_i^2 + B_i^2 + C_i^2 + D_i^2$$

$$A_i^2 = a^2 w_i^2 + b^2 y_i^2 + 2ab w_i y_i$$

$$C_i^2 = c^2 w_i^2 + d^2 y_i^2 + 2cd w_i y_i$$

$$B_i^2 = a^2 x_i^2 + b^2 z_i^2 + 2ab x_i z_i$$

$$D_i^2 = c^2 x_i^2 + d^2 z_i^2 + 2cd x_i z_i$$

(INDEPENDENTLY AT EACH Q)

$$\Sigma_i = \overbrace{(w_i^2 + x_i^2)}^{\text{REF.}}\alpha + \overbrace{(y_i^2 + z_i^2)}^{\text{REF.}}\beta + 2\overbrace{(w_i y_i + x_i z_i)}^{\text{REF.}}\gamma$$

SOLVE FOR UNKNOWNS α, β, AND γ TO GET

$i = 1, 2, 3$

$\alpha = a^2 + c^2$

$\beta = b^2 + d^2$

$\gamma = ab + cd$

$$R_{\text{UNKNOWN}} = \frac{(\beta - \alpha) - 2i\gamma}{2 + \beta + \alpha}$$

FOURIER TRANSFORM OF THE COMPLEX REFLECTION AMPLITUDE

$$\mathcal{R}(z) = \frac{1}{\pi} \mathrm{Re} \int_0^\infty r(k_z) e^{ik_z z} \, dk_z$$

GELFAND LEVITAN MARCHENKO INTEGRAL EQUATION

$$K(z,y) + \mathcal{R}(z+y) + \int_{-z}^{+z} K(z,x) \mathcal{R}(x+y) \, dx = 0$$

SCATTERING LENGTH DENSITY

$$\rho(z) = 2 \frac{d K(z,z)}{dz}$$

GIVEN THE COMPLEX REFLECTION AMPLITUDE, THE SCATTERING LENGTH DENSITY ρ CAN BE OBTAINED FROM AN EXACT, FIRST PRINCIPLE INVERSION FOR A REAL POTENTIAL OF FINITE EXTENT — AND THE SOLUTION IS UNIQUE!

NO FITTING, NO ADJUSTABLE PARAMETERS

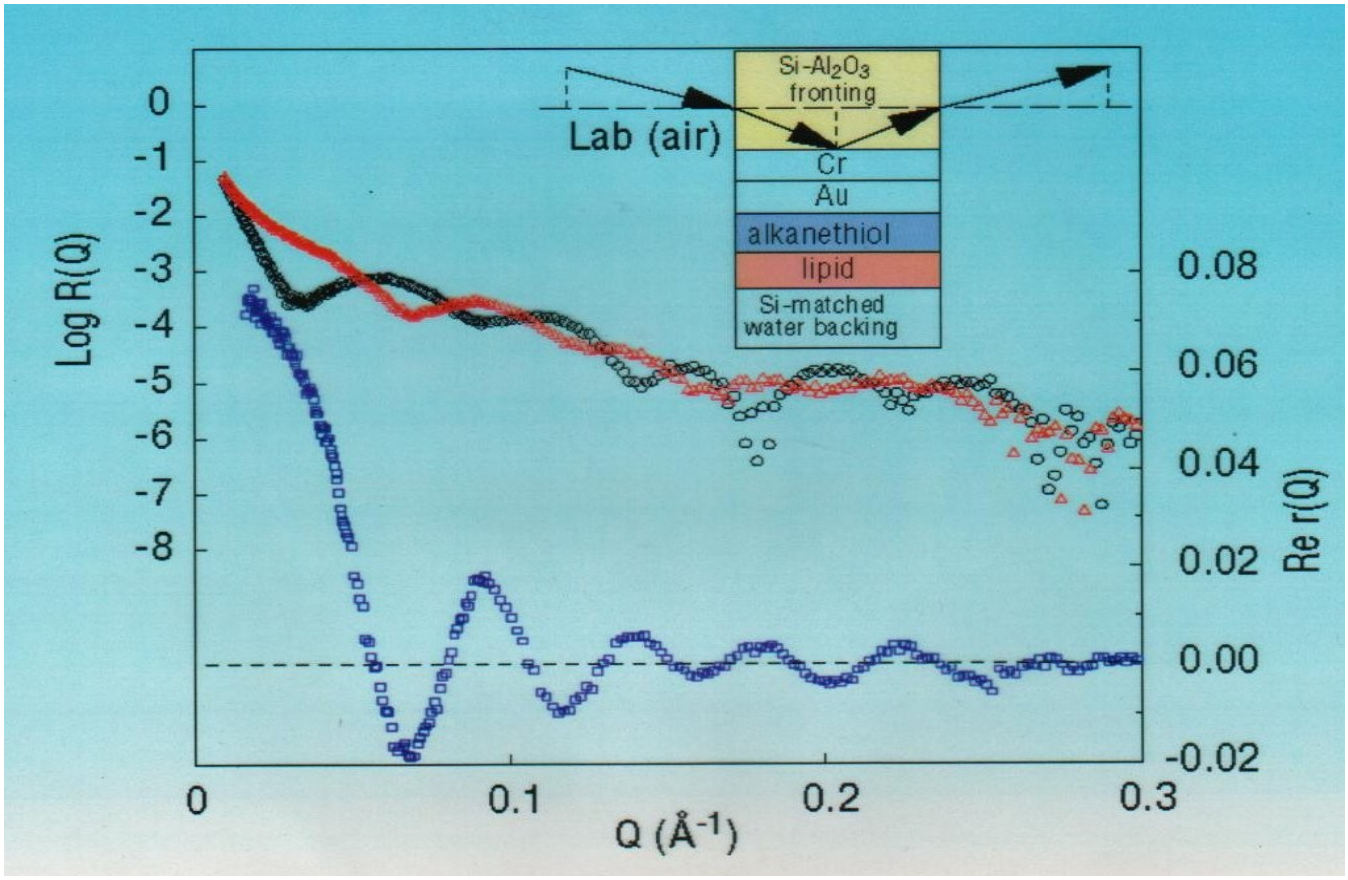
Si-Al2O3 fronting
Lab (air)
Cr
Au
alkanethiol
lipid
Si-matched water backing
Log R(Q)
Re r(Q)
Q (Å-1)
0
-1
-2
-3
-4
-5
-6
-7
-8
0.08
0.06
0.04
0.02
0.00
-0.02
0
0.1
0.2
0.3

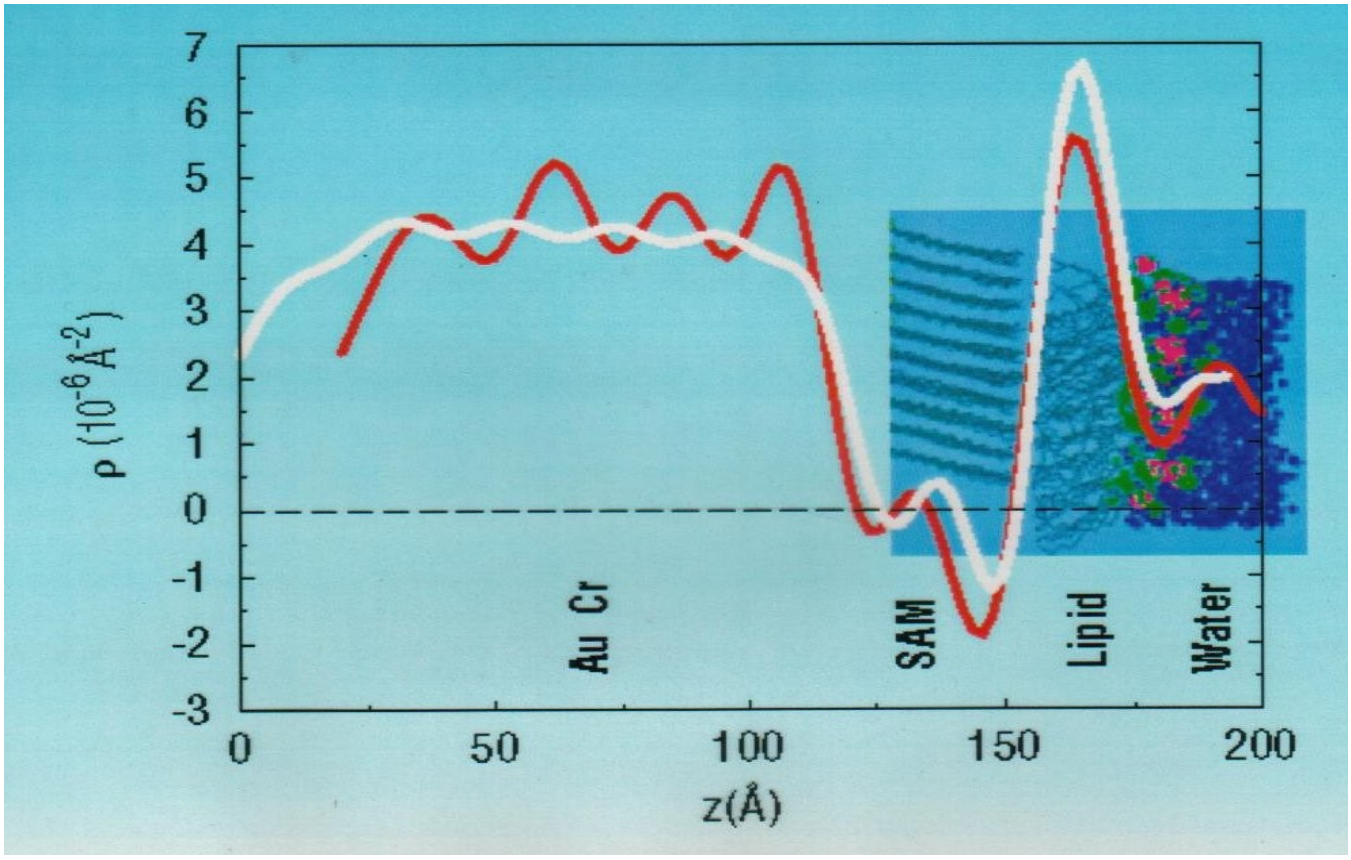
ρ (10-6 Å-2)
z(Å)
Au Cr
SAM
Lipid
Water
7
6
5
4
3
2
1
0
-1
-2
-3
0
50
100
150
200

Optics, 3rd Ed., by E. Hecht, Addison-Wesley, 1998.

Neutron Optics, by V.F. Sears, Oxford University Press, 1989.

Principles of Optics, 6th Ed., by M. Born and E. Wolf,
Pergamon Press, 1987.

Quantum Mechanics, 2nd Ed., by E. Merzbacher, Wiley, 1970.

"Structural Investigations of Membranes in Biology by Neutron Reflectometry", C.F.Majkrzak, N.F.Berk, S.Krueger, and U.A.Perez-Salas, Chapter 12 in *Neutron Scattering in Biology*, Edited by J.Fitter, T.Gutberlet, and J.Katsaras, (Springer, Berlin, 2006) p.225-263.

"Polarized Neutron Reflectometry", C.F.Majkrzak, K.V.O'Donovan, and N.F.Berk, Chapter 9 in *Neutron Scattering from Magnetic Materials*, Edited by T.Chatterji, (Elsevier, Amsterdam, 2006) p.397-471.

"Phase-Sensitive Neutron Reflectometry", C.F.Majkrzak, N.F.Berk, and U.A.Perez-Salas,
Langmuir **19**, 7796 – 7810 (2003).

B.J.Kirby et al., Phase-sensitive specular neutron reflectometry . . ., *Current Opinion in Colloid & Interface Science* **17** (2012) 44-53.

C.F.Majkrzak et al., *J. Appl. Phys.* **110** (2011).

www.ncnr.nist.gov -- look here for information about neutron reflectometry in general as well as in specific studies highlighted in past and current annual reports for the facility.